

Constrained Attack-Resilient Estimation of Stochastic Cyber-Physical Systems

Wenbin Wan ^{a,*}, Hunmin Kim ^a, Naira Hovakimyan ^a, Petros Voulgaris ^b

^aUniversity of Illinois at Urbana-Champaign, USA

^bUniversity of Nevada, Reno, USA

Abstract

In this paper, a constrained attack-resilient estimation algorithm (**CARE**) is developed for stochastic cyber-physical systems. The proposed **CARE** has improved estimation accuracy and detection performance when physical constraints and operational limitations are available. In particular, **CARE** is designed for simultaneous input and state estimation that provides minimum-variance unbiased estimates, and these estimates are projected onto the constrained space restricted by inequality constraints subsequently. We prove that the estimation errors and their covariances from **CARE** are less than those from unconstrained algorithms, and confirm that this property can further reduce the false negative rate in attack detection. We show that estimation errors of **CARE** are practically exponentially stable in mean square. Finally, an illustrative example of attacks on a vehicle is given to demonstrate the improved estimation accuracy and detection performance compared to an existing unconstrained algorithm.

Key words: Cyber-physical systems security; Unknown input estimation; Filter stability; Estimation theory

1 Introduction

Cyber-Physical Systems (CPS) play a vital role in the metabolism of applications from large-scale industrial systems to critical infrastructures, such as smart grids, transportation networks, precision agriculture, and industrial control systems (Rajkumar et al., 2010). Recent developments of CPS and their safety-critical applications have led to a renewed interest in CPS security. The interaction between information technology and the physical system has made control components of CPS vulnerable to malicious attacks (Cárdenas et al., 2008). Recent cases of CPS attacks have clearly illustrated their susceptibility and raised awareness of the security challenges in these systems. These include attacks on large-scale critical infrastructures, such as the StuxNet virus attack on an industrial supervisory control and data acquisition (SCADA) system (Langner, 2011), the German steel mill cyber attack (Lee et al., 2014), and Maroochy Water breach (Slay and Miller, 2007). Similarly,

malicious attacks on avionics and automotive vehicles have been reported, such as the U.S. drone RQ-170 captured in Iran (Peterson and Faramarzi, 2011), and disabling the brakes and stopping the engine on civilian cars (Koscher et al., 2010; Checkoway et al., 2011).

Related work. Traditionally, most works in the field of attack detection had only focused on monitoring the cyber-space misbehavior (Raiyn, 2014). With the emergence of CPS, it becomes vitally important to monitor the physical misbehavior as well, because the impact of the attack on physical systems also needs to be addressed (Cardenas et al., 2008). In the last decade, attention has been drawn from the perspective of the control theory that exploits some prior information of the system dynamics for attack detection and attack-resilient control. For instance, a unified modeling framework for CPS and attacks is proposed in Pasqualetti et al. (2013). A typical control architecture for the networked system under both cyber and physical attacks is proposed in Teixeira et al. (2012); then attack scenarios, such as Denial-of-Service (DoS), false-data injection, and zero dynamics attacks are analyzed using this control architecture in Teixeira et al. (2015).

In recent years, model-based detection has been tremendously studied. Attack detection has been formulated

* Corresponding author.

Email addresses: wenbinw2@illinois.edu (Wenbin Wan), hunmin@illinois.edu (Hunmin Kim), nhovakim@illinois.edu (Naira Hovakimyan), pvoulgaris@unr.edu (Petros Voulgaris).

as an ℓ_0/ℓ_∞ optimization problem, which is NP-hard (Fawzi et al., 2014; Pajic et al., 2014, 2017). A convex relaxation has been studied in Fawzi et al. (2014); Pajic et al. (2017). Furthermore, the worst-case estimation error has been analyzed in Pajic et al. (2017). A residual-based detector has been designed for power systems against false-data injection attacks, and the impact of attacks has been analyzed in Liu et al. (2011). A multi-rate controller to detect zero-dynamic attacks has been designed in Jafarnejadsani et al. (2018). In addition, some papers have studied active detection, such as Mo and Sinopoli (2009); Mo et al. (2014), where the control input is watermarked with a pre-designed scheme that sacrifices optimality. The aforementioned methods have the problem that the state estimate is not resilient concerning the attack signal, and incorrect state estimates make it more challenging for defenders to react to malicious attacks consequently.

Attack-resilient estimation and detection problems have been studied to address the above challenge in Yong et al. (2015a); Forti et al. (2016); Kim et al. (2020), where attack detection has been formulated as a simultaneous input and state estimation problem, and the minimum-variance unbiased estimation technique has been applied. More specifically, the approach has been applied to linear stochastic systems in Yong et al. (2015a), stochastic random set methods in Forti et al. (2016), and nonlinear systems in Kim et al. (2020). These detection algorithms rely on statistical thresholds, such as the χ^2 test which is widely used in the attack detection (Mo et al., 2014; Teixeira et al., 2010). Since the detection accuracy improves when the covariance decreases, a smaller covariance is desired.

On top of the minimum-variance estimation approach, the covariance can be further reduced when we incorporate the information of the input and state in terms of constraints. There have been several investigations on Kalman filtering with state constraints (Simon and Chia, 2002; Julier and LaViola, 2007; Ko and Bitmead, 2007; Simon, 2010). The state constraints are induced by unmodeled dynamics and operational processes. Some of these examples include vision-aided inertial navigation (Mourikis and Roumeliotis, 2007), target tracking (Wang et al., 2002) and power systems (Yong et al., 2015b; Wood et al., 2013). Constraints on inputs are also considered, such as avoiding reachable dangerous states under the assumption that the attack input is constrained (Kafash et al., 2018) and designing a resilient controller based on the partial knowledge of the attacker in terms of inequality constraints (Djouadi et al., 2015). The methods in Kafash et al. (2018); Djouadi et al. (2015) can efficiently be used to maneuver a class of attacks when input inequality constraints are available, but cannot resiliently address the estimation problem due to the false-data injection. This problem remains to be solved with a stability guarantee in the presence of inequality constraints. In the current paper,

we aim to solve the resilient estimation problem and investigate the stability and performance of the algorithm design that integrates with information aggregation. To the best of our knowledge, this is the first investigation that considers both state and input inequality constraints for attack-resilient estimation with guaranteed stability.

Contributions. We propose a constrained attack-resilient estimation algorithm (CARE) of linear discrete-time stochastic systems with information aggregation, where both input and state inequality constraints are considered. The proposed CARE consists of an optimal estimation part and an information aggregation step. The optimal estimation provides minimum-variance unbiased estimates, and then these optimal estimates are projected onto the constrained space in the information aggregation step. We provide rigorous analysis that CARE reduces the input and state estimation errors, their error covariances, and the false negative rate in attack detection. Furthermore, we investigate the stability of the estimation errors in the presence of the input and state inequality constraints. Since the estimates are potentially biased after the projection is applied, the traditional stability analysis for unbiased estimation becomes invalid. In this context, we prove that estimation errors of CARE are practically exponentially stable in mean square after the projection. An illustrative example of attacks on a vehicle shows the performance of the proposed algorithm.

A preliminary version of this paper appeared in Wan et al. (2019). The current paper is significantly extended from the preliminary version. First, we complete technical proofs of all theorems and lemmas and confirm the reduction of the false negative rate in attack detection when the proposed algorithm is applied. In addition, we provide a comprehensive overview of methods of attack detection and attack-resilient estimation for CPS and further insights into the attack-resilient approaches with various constraints. Finally, we provide an example of attack estimation and detection on a vehicle showing the effectiveness and improvement of the proposed constrained attack-resilient estimation algorithm.

Paper organization. The rest of the paper is organized as follows. Section 2 introduces notations, χ^2 test for detection, and problem formulation. The high-level idea of the proposed algorithm is presented in Section 3.1. Section 3.2 gives a detailed algorithm derivation. Section 4 demonstrates the performance improvement and investigates stability analysis of the proposed algorithm. Section 5 presents an illustrative example of vehicle attacks. Finally, Section 6 draws the conclusion.

2 Preliminaries

2.1 Notations

We use the subscript k to denote the time index. For a real set \mathbb{R} , \mathbb{R}_+^n denotes the set of positive elements in the n -dimensional Euclidean space, and $\mathbb{R}^{n \times m}$ denotes the set of all $n \times m$ real matrices. For a matrix \mathbf{A} , \mathbf{A}^\top , \mathbf{A}^{-1} , \mathbf{A}^\dagger , $\text{diag}(\mathbf{A})$, $\text{tr}(\mathbf{A})$ and $\text{rank}(\mathbf{A})$ denote the transpose, inverse, Moore-Penrose pseudoinverse, diagonal, trace and rank of \mathbf{A} , respectively. For a symmetric matrix \mathbf{S} , $\mathbf{S} > 0$ ($\mathbf{S} \geq 0$) indicates that \mathbf{S} is positive (semi)definite. The matrix \mathbf{I} denotes the identity matrix with an appropriate dimension. We use $\|\cdot\|$ to denote the standard Euclidean norm for vector or an induced matrix norm if it is not specified, $\mathbb{E}[\cdot]$ to denote the expectation operator, and \times to denote matrix multiplication when the multiplied terms are in different lines. For a vector \mathbf{a} , $\mathbf{a}(i)$ denotes the i^{th} element in the vector \mathbf{a} . Finally, vectors \mathbf{a} , $\hat{\mathbf{a}}$, $\tilde{\mathbf{a}} \triangleq \mathbf{a} - \hat{\mathbf{a}}$ denote the ground truth, estimate and estimation error of \mathbf{a} , respectively.

2.2 χ^2 Test for Detection

The χ^2 test is widely used in attack detection for stochastic systems (Teixeira et al., 2010; Mo et al., 2014). Given a sample of Gaussian random variable $\hat{\boldsymbol{\sigma}}_k$ with unknown mean $\boldsymbol{\sigma}_k$ and known covariance $\boldsymbol{\Sigma}_k$, the χ^2 test provides statistical evidence of whether $\boldsymbol{\sigma}_k = 0$ or not. In particular, the sample $\hat{\boldsymbol{\sigma}}_k$ is being normalized by $\hat{\boldsymbol{\sigma}}_k^\top \boldsymbol{\Sigma}_k^{-1} \hat{\boldsymbol{\sigma}}_k$, and we compare the normalized value with $\chi_{df}^2(\alpha)$, where $\chi_{df}^2(\alpha)$ is the χ^2 value with degree of freedom df and statistical significance level α . We reject the null hypothesis $H_0: \boldsymbol{\sigma}_k = 0$, if $\hat{\boldsymbol{\sigma}}_k^\top \boldsymbol{\Sigma}_k^{-1} \hat{\boldsymbol{\sigma}}_k > \chi_{df}^2(\alpha)$, and accept alternative hypothesis $H_1: \boldsymbol{\sigma}_k \neq 0$, i.e., there is significant statistical evidence that $\boldsymbol{\sigma}_k$ is non-zero. Otherwise, we accept the null hypothesis H_0 , i.e., there is no significant evidence that $\boldsymbol{\sigma}_k$ is non-zero.

False negative rate. Given a set of vectors $\{\boldsymbol{\sigma}_k\}$, the false negative rate of the χ^2 test is defined as the ratio of the number of false negative test results N_{neg} and the number of nonzero vectors in the given set $N_{\boldsymbol{\sigma}_k \neq 0}$

$$F_{neg}(\{\hat{\boldsymbol{\sigma}}_k\}, \{\boldsymbol{\Sigma}_k\}) \triangleq \frac{N_{neg}}{N_{\boldsymbol{\sigma}_k \neq 0}} = \frac{\sum_k(\mathbf{1}_k)}{N_{\boldsymbol{\sigma}_k \neq 0}}, \quad (1)$$

where

$$\mathbf{1}_k \triangleq \begin{cases} 1, & \text{if } \hat{\boldsymbol{\sigma}}_k^\top \boldsymbol{\Sigma}_k^{-1} \hat{\boldsymbol{\sigma}}_k \leq \chi_{df}^2(\alpha) \text{ and } \boldsymbol{\sigma}_k \neq 0 \\ 0, & \text{otherwise} \end{cases}. \quad (2)$$

2.3 Problem Formulation

Consider the following linear time-varying (LTV) discrete-time stochastic system¹

$$\begin{aligned} \mathbf{x}_{k+1} &= \mathbf{A}_k \mathbf{x}_k + \mathbf{B}_k \mathbf{u}_k + \mathbf{G}_k \mathbf{d}_k + \mathbf{w}_k \\ \mathbf{y}_k &= \mathbf{C}_k \mathbf{x}_k + \mathbf{v}_k, \end{aligned} \quad (3)$$

where $\mathbf{x}_k \in \mathbb{R}^m$, $\mathbf{u}_k \in \mathbb{R}^n$ and $\mathbf{y}_k \in \mathbb{R}^{n_y}$ are the state, the control input and the sensor measurement, respectively. The attack signal is modeled as a simultaneous input $\mathbf{d}_k \in \mathbb{R}^{n_d}$, which is unknown to the defender. System matrices \mathbf{A}_k , \mathbf{B}_k , \mathbf{C}_k and \mathbf{G}_k are known and bounded with appropriate dimensions. The process noise \mathbf{w}_k and the measurement noise \mathbf{v}_k are assumed to be i.i.d. Gaussian random variables with zero means and covariances $\mathbf{Q}_k \triangleq \mathbb{E}[\mathbf{w}_k \mathbf{w}_k^\top] \geq 0$ and $\mathbf{R}_k \triangleq \mathbb{E}[\mathbf{v}_k \mathbf{v}_k^\top] > 0$. Moreover, the measurement noise \mathbf{v}_k , the process noise \mathbf{w}_k , and the initial state \mathbf{x}_0 are uncorrelated with each other.

In the cyber-space, digital attack signals could be unconstrained, but their impact on the physical world is restricted by physical and operational constraints (i.e., \mathbf{x}_k and \mathbf{d}_k are constrained). Any physical constraints and ability limitations on attack signals and states are presented by known inequality constraints

$$\mathbf{A}_k \mathbf{d}_k \leq \mathbf{b}_k, \quad \mathbf{B}_k \mathbf{x}_k \leq \mathbf{c}_k, \quad (4)$$

where matrices \mathbf{A}_k , \mathbf{B}_k , and vectors \mathbf{b}_k , \mathbf{c}_k are known and bounded with appropriate dimensions. Throughout this paper, we assume that the feasible sets of the constraints in (4) are non-empty.

Problem statement. Given the LTV discrete-time stochastic system in (3), we aim to design an attack-resilient estimation algorithm that can simultaneously estimate the system state \mathbf{x}_k and the attack signal \mathbf{d}_k . In addition, we seek to improve estimation accuracy and detection performance with stability guarantee when incorporating the information of the input and state in terms of constraints in (4).

3 Algorithm Design

To address the problem statement described in Section 2.3, we propose a constrained attack-resilient estimation algorithm (CARE), as sketched in Fig. 1, which consists of an optimal estimation part and an information aggregation step via projection. In particular, the optimal estimation provides unbiased minimum-variance estimates, and these estimates are projected

¹ The current paper considers a general formulation for the attack input matrix \mathbf{G}_k . If \mathbf{d}_k is injected into the control input, then $\mathbf{G}_k = \mathbf{B}_k$. If \mathbf{d}_k is directly injected into the system, then $\mathbf{G}_k = \mathbf{I}$.

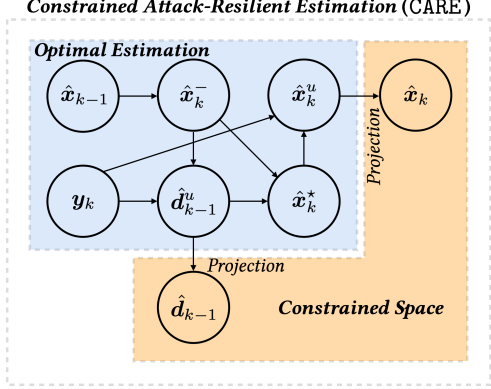


Fig. 1. Constrained Attack-Resilient Estimation (CARE).

onto the constrained space eventually in the information aggregation step. We outline the essential steps of CARE in Section 3.1 and provide a detailed derivation of the algorithm in Section 3.2.

3.1 Algorithm Statement

The proposed CARE can be summarized as follows:

(1) *prediction*:

$$\hat{\mathbf{x}}_k^- = \mathbf{A}_{k-1}\hat{\mathbf{x}}_{k-1} + \mathbf{B}_{k-1}\mathbf{u}_{k-1}; \quad (5)$$

(2) *attack estimation*:

$$\hat{\mathbf{d}}_{k-1}^u = \mathbf{M}_k(\mathbf{y}_k - \mathbf{C}_k\hat{\mathbf{x}}_k^-); \quad (6)$$

(3) *time update*:

$$\hat{\mathbf{x}}_k^* = \hat{\mathbf{x}}_k^- + \mathbf{G}_{k-1}\hat{\mathbf{d}}_{k-1}^u; \quad (7)$$

(4) *measurement update*:

$$\hat{\mathbf{x}}_k^u = \hat{\mathbf{x}}_k^* + \mathbf{L}_k(\mathbf{y}_k - \mathbf{C}_k\hat{\mathbf{x}}_k^*); \quad (8)$$

(5) *projection update*:

$$\begin{aligned} \hat{\mathbf{d}}_{k-1} &= \arg \min_{\mathbf{d}} (\mathbf{d} - \hat{\mathbf{d}}_{k-1}^u)^\top (\mathbf{P}_{k-1}^{d,u})^{-1} (\mathbf{d} - \hat{\mathbf{d}}_{k-1}^u) \\ &\text{subject to } \mathcal{A}_{k-1}\mathbf{d} \leq \mathbf{b}_{k-1}; \end{aligned} \quad (9)$$

$$\begin{aligned} \hat{\mathbf{x}}_k &= \arg \min_{\mathbf{x}} (\mathbf{x} - \hat{\mathbf{x}}_k^u)^\top (\mathbf{P}_k^{x,u})^{-1} (\mathbf{x} - \hat{\mathbf{x}}_k^u) \\ &\text{subject to } \mathcal{B}_k\mathbf{x} \leq \mathbf{c}_k. \end{aligned} \quad (10)$$

Given the previous state estimate $\hat{\mathbf{x}}_{k-1}$ and its error covariance $\mathbf{P}_{k-1}^x \triangleq \mathbb{E}[\tilde{\mathbf{x}}_{k-1}(\tilde{\mathbf{x}}_{k-1})^\top]$, the current state can be predicted by $\hat{\mathbf{x}}_k^-$ in (5) under the assumption that the attack signal \mathbf{d}_{k-1} is absent. The unconstrained attack estimate $\hat{\mathbf{d}}_{k-1}^u$ can be obtained by comparing the difference between the predicted output $\mathbf{C}_k\hat{\mathbf{x}}_k^-$ and the measured output \mathbf{y}_k in (6), where \mathbf{M}_k is the filter gain that

is obtained by minimizing the input error covariances $\mathbf{P}_{k-1}^{d,u}$. The state prediction $\hat{\mathbf{x}}_k^-$ can be updated incorporating the unconstrained attack estimate $\hat{\mathbf{d}}_{k-1}^u$ in (7). The output \mathbf{y}_k is used to correct the current state estimate in (8), where \mathbf{L}_k is the filter gain that is obtained by minimizing the state error covariance $\mathbf{P}_k^{x,u}$. In the information aggregation step (projection update), we apply the input constraint in (9) by projecting $\hat{\mathbf{d}}_{k-1}^u$ onto the constrained space and obtain the constrained attack estimate $\hat{\mathbf{d}}_{k-1}$. Similarly, the state constraint in (10) is applied to obtain the constrained state estimate $\hat{\mathbf{x}}_k$. The complete algorithm is presented in Algorithm 1.

Algorithm 1 Constrained Attack-Resilient Estimation:

$$[\hat{\mathbf{d}}_{k-1}, \mathbf{P}_{k-1}^d, \hat{\mathbf{x}}_k, \mathbf{P}_k^x] = \text{CARE}(\hat{\mathbf{x}}_{k-1}, \mathbf{P}_{k-1}^x)$$

▷ Prediction

$$1: \hat{\mathbf{x}}_k^- = \mathbf{A}_{k-1}\hat{\mathbf{x}}_{k-1} + \mathbf{B}_{k-1}\mathbf{u}_{k-1};$$

$$2: \mathbf{P}_k^{x,-} = \mathbf{A}_{k-1}\mathbf{P}_{k-1}^x\mathbf{A}_{k-1}^\top + \mathbf{Q}_{k-1};$$

▷ Attack estimation

$$3: \tilde{\mathbf{R}}_k = (\mathbf{C}_k\mathbf{P}_k^{x,-}\mathbf{C}_k^\top + \mathbf{R}_k)^{-1};$$

$$4: \mathbf{M}_k = (\mathbf{G}_{k-1}^\top\mathbf{C}_k^\top\tilde{\mathbf{R}}_k\mathbf{C}_k\mathbf{G}_{k-1})^{-1}\mathbf{G}_{k-1}^\top\mathbf{C}_k^\top\tilde{\mathbf{R}}_k;$$

$$5: \hat{\mathbf{d}}_{k-1}^u = \mathbf{M}_k(\mathbf{y}_k - \mathbf{C}_k\hat{\mathbf{x}}_k^-);$$

$$6: \mathbf{P}_{k-1}^{d,u} = (\mathbf{G}_{k-1}^\top\mathbf{C}_k^\top\tilde{\mathbf{R}}_k\mathbf{C}_k\mathbf{G}_{k-1})^{-1};$$

$$7: \mathbf{P}_{k-1}^{xd} = -\mathbf{P}_{k-1}^x\mathbf{A}_{k-1}^\top\mathbf{C}_k^\top\mathbf{M}_k^\top;$$

▷ Time update

$$8: \hat{\mathbf{x}}_k^* = \hat{\mathbf{x}}_k^- + \mathbf{G}_{k-1}\hat{\mathbf{d}}_{k-1}^u;$$

$$9: \mathbf{P}_k^{x*} = \mathbf{A}_{k-1}\mathbf{P}_{k-1}^x\mathbf{A}_{k-1}^\top + \mathbf{A}_{k-1}\mathbf{P}_{k-1}^{xd}\mathbf{G}_{k-1}^\top + \mathbf{G}_{k-1}(\mathbf{P}_{k-1}^{d,u})^\top\mathbf{A}_{k-1}^\top + \mathbf{G}_{k-1}\mathbf{P}_{k-1}^{d,u}\mathbf{G}_{k-1}^\top - \mathbf{G}_{k-1}\mathbf{M}_k\mathbf{C}_k\mathbf{Q}_{k-1} - \mathbf{Q}_{k-1}\mathbf{C}_k^\top\mathbf{M}_k^\top\mathbf{G}_{k-1}^\top + \mathbf{Q}_{k-1};$$

$$10: \tilde{\mathbf{R}}_k^* = \mathbf{C}_k\mathbf{P}_k^{x*}\mathbf{C}_k^\top - \mathbf{C}_k\mathbf{G}_{k-1}\mathbf{M}_k\mathbf{R}_k - \mathbf{R}_k\mathbf{M}_k^\top\mathbf{G}_{k-1}^\top\mathbf{C}_k^\top + \mathbf{R}_k;$$

▷ Measurement update

$$11: \mathbf{L}_k = (\mathbf{P}_k^{x*}\mathbf{C}_k^\top - \mathbf{G}_{k-1}\mathbf{M}_k\mathbf{R}_k)\tilde{\mathbf{R}}_k^{*\dagger};$$

$$12: \hat{\mathbf{x}}_k^u = \hat{\mathbf{x}}_k^* + \mathbf{L}_k(\mathbf{y}_k - \mathbf{C}_k\hat{\mathbf{x}}_k^*);$$

$$13: \mathbf{P}_k^{x,u} = (\mathbf{I} - \mathbf{L}_k\mathbf{C}_k)\mathbf{G}_{k-1}\mathbf{M}_k\mathbf{R}_k\mathbf{L}_k^\top + \mathbf{L}_k\mathbf{R}_k\mathbf{M}_k^\top\mathbf{G}_{k-1}^\top(\mathbf{I} - \mathbf{L}_k\mathbf{C}_k)^\top + (\mathbf{I} - \mathbf{L}_k\mathbf{C}_k)\mathbf{P}_k^{x*}(\mathbf{I} - \mathbf{L}_k\mathbf{C}_k)^\top + \mathbf{L}_k\mathbf{R}_k\mathbf{L}_k^\top;$$

▷ Projection update

$$14: \gamma_{k-1}^d = \mathbf{P}_{k-1}^{d,u}\bar{\mathbf{A}}_{k-1}^\top(\bar{\mathbf{A}}_{k-1}\mathbf{P}_{k-1}^{d,u}\bar{\mathbf{A}}_{k-1}^\top)^{-1};$$

$$15: \hat{\mathbf{d}}_{k-1} = \hat{\mathbf{d}}_{k-1}^u - \gamma_{k-1}^d(\bar{\mathbf{A}}_{k-1}\hat{\mathbf{d}}_{k-1}^u - \bar{\mathbf{b}}_{k-1});$$

$$16: \mathbf{P}_{k-1}^d = (\mathbf{I} - \gamma_{k-1}^d\bar{\mathbf{A}}_{k-1})\mathbf{P}_{k-1}^{d,u}(\mathbf{I} - \gamma_{k-1}^d\bar{\mathbf{A}}_{k-1})^\top;$$

$$17: \gamma_k^x = \mathbf{P}_k^{x,u}\bar{\mathbf{B}}_k^\top(\bar{\mathbf{B}}_k\mathbf{P}_k^{x,u}\bar{\mathbf{B}}_k^\top)^{-1};$$

$$18: \hat{\mathbf{x}}_k = \hat{\mathbf{x}}_k^u - \gamma_k^x(\bar{\mathbf{B}}_k\hat{\mathbf{x}}_k^u - \bar{\mathbf{c}}_k);$$

$$19: \mathbf{P}_k^x = (\mathbf{I} - \gamma_k^x\bar{\mathbf{B}}_k)\mathbf{P}_k^{x,u}(\mathbf{I} - \gamma_k^x\bar{\mathbf{B}}_k)^\top;$$

3.2 Algorithm Derivation

Prediction. The current state can be predicted by (5) under the assumption that the attack signal $\mathbf{d}_{k-1} = 0$. The prediction error covariance is

$$\mathbf{P}_k^{x,-} \triangleq \mathbb{E}[\tilde{\mathbf{x}}_k^-(\tilde{\mathbf{x}}_k^-)^\top] = \mathbf{A}_{k-1}\mathbf{P}_{k-1}^x\mathbf{A}_{k-1}^\top + \mathbf{Q}_{k-1}.$$

Attack estimation. The linear attack estimator in (6) utilizes the difference between the measured out-

put \mathbf{y}_k and the predicted output $\mathbf{C}_k \hat{\mathbf{x}}_k^-$. Substituting (3) and (5) into (6), we have

$$\hat{\mathbf{d}}_{k-1}^u = \mathbf{M}_k (\mathbf{C}_k \mathbf{A}_{k-1} \tilde{\mathbf{x}}_{k-1} + \mathbf{C}_k \mathbf{G}_{k-1} \mathbf{d}_{k-1} + \mathbf{C}_k \mathbf{w}_{k-1} + \mathbf{v}_k),$$

which is a linear function of the attack signal \mathbf{d}_{k-1} . Applying the method of least squares (Sayed, 2003), which gives linear minimum-variance unbiased estimates, we can get the optimal gain

$$\mathbf{M}_k = (\mathbf{G}_{k-1}^\top \mathbf{C}_k^\top \tilde{\mathbf{R}}_k \mathbf{C}_k \mathbf{G}_{k-1})^{-1} \mathbf{G}_{k-1}^\top \mathbf{C}_k^\top \tilde{\mathbf{R}}_k,$$

where $\tilde{\mathbf{R}}_k \triangleq (\mathbf{C}_k \mathbf{P}_k^{x,-} \mathbf{C}_k + \mathbf{R}_k)^{-1}$. The error covariance can be found by

$$\mathbf{P}_{k-1}^{d,u} = \mathbf{M}_k \tilde{\mathbf{R}}_k^{-1} \mathbf{M}_k^\top = (\mathbf{G}_{k-1}^\top \mathbf{C}_k^\top \tilde{\mathbf{R}}_k \mathbf{C}_k \mathbf{G}_{k-1})^{-1}.$$

The cross error covariance of the state estimate and the attack estimate is

$$\mathbf{P}_{k-1}^{xd} = -\mathbf{P}_{k-1}^x \mathbf{A}_{k-1}^\top \mathbf{C}_k^\top \mathbf{M}_k^\top.$$

Time update. Given the unconstrained attack estimate $\hat{\mathbf{d}}_{k-1}^u$, the state prediction $\hat{\mathbf{x}}_k^-$ can be updated as in (7). We derive the error covariance of $\hat{\mathbf{x}}_k^*$ as

$$\begin{aligned} \mathbf{P}_k^{x*} &\triangleq \mathbb{E}[\tilde{\mathbf{x}}_k^* (\tilde{\mathbf{x}}_k^*)^\top] \\ &= \mathbf{A}_{k-1} \mathbf{P}_{k-1}^x \mathbf{A}_{k-1}^\top + \mathbf{A}_{k-1} \mathbf{P}_{k-1}^{xd} \mathbf{G}_{k-1}^\top \\ &\quad + \mathbf{G}_{k-1} \mathbf{P}_{k-1}^{dx} \mathbf{A}_{k-1}^\top + \mathbf{G}_{k-1} \mathbf{P}_{k-1}^{d,u} \mathbf{G}_{k-1}^\top + \mathbf{Q}_{k-1} \\ &\quad - \mathbf{G}_{k-1} \mathbf{M}_k \mathbf{C}_k \mathbf{Q}_{k-1} - \mathbf{Q}_{k-1} \mathbf{C}_k^\top \mathbf{M}_k^\top \mathbf{G}_{k-1}^\top, \end{aligned}$$

where $\mathbf{P}_{k-1}^{dx} = (\mathbf{P}_{k-1}^{xd})^\top$.

Measurement update. In this step, the measurement \mathbf{y}_k is used to update the propagated estimate $\hat{\mathbf{x}}_k^*$ as shown in (8). The covariance of the state estimation error is

$$\begin{aligned} \mathbf{P}_k^{x,u} &\triangleq \mathbb{E}[(\tilde{\mathbf{x}}_k^u) (\tilde{\mathbf{x}}_k^u)^\top] \\ &= (\mathbf{I} - \mathbf{L}_k \mathbf{C}_k) \mathbf{G}_{k-1} \mathbf{M}_k \mathbf{R}_k \mathbf{L}_k^\top + \mathbf{L}_k \mathbf{R}_k \mathbf{L}_k^\top \\ &\quad + \mathbf{L}_k \mathbf{R}_k \mathbf{M}_k^\top \mathbf{G}_{k-1}^\top (\mathbf{I} - \mathbf{L}_k \mathbf{C}_k)^\top \\ &\quad + (\mathbf{I} - \mathbf{L}_k \mathbf{C}_k) \mathbf{P}_k^{x*} (\mathbf{I} - \mathbf{L}_k \mathbf{C}_k)^\top. \end{aligned}$$

The gain matrix \mathbf{L}_k is obtained by minimizing the trace of $\mathbf{P}_k^{x,u}$, i.e.

$$\min_{\mathbf{L}_k} \text{tr}(\mathbf{P}_k^{x,u}). \quad (11)$$

The solution of (11) is given by

$$\mathbf{L}_k = (\mathbf{P}_k^{x*} \mathbf{C}_k^\top - \mathbf{G}_{k-1} \mathbf{M}_k \mathbf{R}_k) \tilde{\mathbf{R}}_k^{\star\top},$$

where $\tilde{\mathbf{R}}_k^{\star} \triangleq \mathbf{C}_k \mathbf{P}_k^{x*} \mathbf{C}_k^\top + \mathbf{R}_k - \mathbf{C}_k \mathbf{G}_{k-1} \mathbf{M}_k \mathbf{R}_k - \mathbf{R}_k \mathbf{M}_k^\top \mathbf{G}_{k-1}^\top \mathbf{C}_k^\top$.

Projection update. We are now in the position to project the estimates onto the constrained space. Apply the first constraint in (4) to the unconstrained attack estimate $\hat{\mathbf{d}}_{k-1}^u$, and the attack estimation problem can be formulated as the following constrained convex optimization problem

$$\begin{aligned} \hat{\mathbf{d}}_{k-1} &= \arg \min_{\mathbf{d}} (\mathbf{d} - \hat{\mathbf{d}}_{k-1}^u)^\top \mathbf{W}_{k-1}^d (\mathbf{d} - \hat{\mathbf{d}}_{k-1}^u) \\ &\text{subject to } \mathcal{A}_{k-1} \mathbf{d} \leq \mathbf{b}_{k-1}, \end{aligned} \quad (12)$$

where \mathbf{W}_{k-1}^d can be any positive definite symmetric weighting matrix. In the current paper, we select $\mathbf{W}_{k-1}^d = (\mathbf{P}_{k-1}^{d,u})^{-1}$ which results in the smallest error covariance as shown in Simon and Chia (2002). From Karush-Kuhn-Tucker (KKT) conditions of optimality, we can find the corresponding active constraints. We denote $\bar{\mathcal{A}}_k$ and $\bar{\mathbf{b}}_k$ the rows of \mathcal{A}_k and the elements of \mathbf{b}_k corresponding to the active constraints of $\mathcal{A}_{k-1} \mathbf{d} \leq \mathbf{b}_{k-1}$. Then (12) becomes

$$\begin{aligned} \hat{\mathbf{d}}_{k-1} &= \arg \min_{\mathbf{d}} (\mathbf{d} - \hat{\mathbf{d}}_{k-1}^u)^\top (\mathbf{P}_{k-1}^{d,u})^{-1} (\mathbf{d} - \hat{\mathbf{d}}_{k-1}^u) \\ &\text{subject to } \bar{\mathcal{A}}_{k-1} \mathbf{d} = \bar{\mathbf{b}}_{k-1}. \end{aligned} \quad (13)$$

The solution of (13) can be found by

$$\hat{\mathbf{d}}_{k-1} = \hat{\mathbf{d}}_{k-1}^u - \gamma_{k-1}^d (\bar{\mathcal{A}}_{k-1} \hat{\mathbf{d}}_{k-1}^u - \bar{\mathbf{b}}_{k-1}),$$

where

$$\gamma_{k-1}^d \triangleq \mathbf{P}_{k-1}^{d,u} \bar{\mathcal{A}}_{k-1}^\top (\bar{\mathcal{A}}_{k-1} \mathbf{P}_{k-1}^{d,u} \bar{\mathcal{A}}_{k-1}^\top)^{-1}. \quad (14)$$

The attack estimation error is

$$\begin{aligned} \tilde{\mathbf{d}}_{k-1} &= (\mathbf{I} - \gamma_{k-1}^d \bar{\mathcal{A}}_{k-1}) \tilde{\mathbf{d}}_{k-1}^u + \gamma_{k-1}^d (\bar{\mathcal{A}}_{k-1} \mathbf{d}_{k-1} - \bar{\mathbf{b}}_{k-1}) \\ &= \tilde{\mathbf{d}}_{k-1}^u - \gamma_{k-1}^d (\bar{\mathcal{A}}_{k-1} \tilde{\mathbf{d}}_{k-1}^u - \bar{\mathbf{b}}_{k-1}). \end{aligned} \quad (15)$$

The error covariance can be found by

$$\begin{aligned} \mathbf{P}_{k-1}^d &\triangleq \mathbb{E}[\tilde{\mathbf{d}}_{k-1} \tilde{\mathbf{d}}_{k-1}^\top] \\ &= (\mathbf{I} - \gamma_{k-1}^d \bar{\mathcal{A}}_{k-1}) \mathbf{P}_{k-1}^{d,u} (\mathbf{I} - \gamma_{k-1}^d \bar{\mathcal{A}}_{k-1})^\top \end{aligned} \quad (16)$$

under the assumption that $\gamma_{k-1}^d (\bar{\mathcal{A}}_{k-1} \mathbf{d}_{k-1} - \bar{\mathbf{b}}_{k-1}) = 0$ holds. Notice that this assumption holds when the ground truth \mathbf{d}_{k-1} satisfies the active constraint $\bar{\mathcal{A}}_{k-1} \mathbf{d}_{k-1} = \bar{\mathbf{b}}_{k-1}$. From (14), it can be verified that

$\gamma_{k-1}^d \bar{\mathcal{A}}_{k-1} \mathbf{P}_{k-1}^{d,u} = \gamma_{k-1}^d \bar{\mathcal{A}}_{k-1} \mathbf{P}_{k-1}^{d,u} (\gamma_{k-1}^d \bar{\mathcal{A}}_{k-1})^\top$. Therefore, from (16) we have

$$\begin{aligned} \mathbf{P}_{k-1}^d &= \mathbf{P}_{k-1}^{d,u} - \gamma_{k-1}^d \bar{\mathcal{A}}_{k-1} \mathbf{P}_{k-1}^{d,u} - \mathbf{P}_{k-1}^{d,u} (\gamma_{k-1}^d \bar{\mathcal{A}}_{k-1})^\top \\ &\quad + \gamma_{k-1}^d \bar{\mathcal{A}}_{k-1} \mathbf{P}_{k-1}^{d,u} (\gamma_{k-1}^d \bar{\mathcal{A}}_{k-1})^\top \\ &= (\mathbf{I} - \gamma_{k-1}^d \bar{\mathcal{A}}_{k-1}) \mathbf{P}_{k-1}^{d,u}. \end{aligned} \quad (17)$$

Similarly, applying the second constraint in (4) to the unconstrained state estimate $\hat{\mathbf{x}}_k^u$, we formalize the state estimation problem as follows:

$$\begin{aligned} \hat{\mathbf{x}}_k &= \arg \min_{\mathbf{x}} (\mathbf{x} - \hat{\mathbf{x}}_k^u)^\top \mathbf{W}_k^x (\mathbf{x} - \hat{\mathbf{x}}_k^u) \\ &\text{subject to } \mathcal{B}_k \mathbf{x} \leq \mathbf{c}_k, \end{aligned} \quad (18)$$

where we select $\mathbf{W}_k^x = (\mathbf{P}_k^{x,u})^{-1}$ for the smallest error covariance. We denote $\bar{\mathcal{B}}_k$ and $\bar{\mathbf{c}}_k$ the rows of \mathcal{B}_k and the elements of \mathbf{c}_k corresponding to the active constraints of $\mathcal{B}_k \mathbf{x} \leq \mathbf{c}_k$. Using the active constraints, we reformulate (18) as follows:

$$\begin{aligned} \hat{\mathbf{x}}_k &= \arg \min_{\mathbf{x}} (\mathbf{x} - \hat{\mathbf{x}}_k^u)^\top (\mathbf{P}_k^{x,u})^{-1} (\mathbf{x} - \hat{\mathbf{x}}_k^u) \\ &\text{subject to } \bar{\mathcal{B}}_k \mathbf{x} = \bar{\mathbf{c}}_k. \end{aligned} \quad (19)$$

The solution of (19) is given by

$$\hat{\mathbf{x}}_k = \hat{\mathbf{x}}_k^u - \gamma_k^x (\bar{\mathcal{B}}_k \hat{\mathbf{x}}_k^u - \bar{\mathbf{c}}_k),$$

where

$$\gamma_k^x \triangleq \mathbf{P}_k^{x,u} \bar{\mathcal{B}}_k^\top (\bar{\mathcal{B}}_k \mathbf{P}_k^{x,u} \bar{\mathcal{B}}_k^\top)^{-1}. \quad (20)$$

Under the assumption that $\gamma_k^x (\bar{\mathcal{B}}_k \hat{\mathbf{x}}_k^u - \bar{\mathbf{c}}_k) = 0$ holds, the state estimation error covariance can be expressed as

$$\mathbf{P}_k^x = \bar{\Gamma}_k \mathbf{P}_k^{x,u} \bar{\Gamma}_k^\top, \quad (21)$$

where $\bar{\Gamma}_k \triangleq \mathbf{I} - \gamma_k^x \bar{\mathcal{B}}_k$. Notice that this assumption holds when the ground truth \mathbf{x}_k satisfies the active constraint $\bar{\mathcal{B}}_k \mathbf{x}_k = \bar{\mathbf{c}}_k$.

4 Performance and Stability Analysis

In Section 4.1, we show that the projection induced by inequality constraints improves attack-resilient estimation accuracy and detection performance by decreasing estimation errors and the false negative rate in attack detection. Notice that the estimate $\hat{\mathbf{d}}_{k-1}$ and the ground truth \mathbf{d}_{k-1} satisfy the active constraint $\bar{\mathcal{A}}_{k-1} \hat{\mathbf{d}}_{k-1} - \bar{\mathbf{b}}_{k-1} = 0$ in (13) and the inequality constraint $\mathcal{A}_{k-1} \mathbf{d}_{k-1} \leq \mathbf{b}_{k-1}$ in (4), respectively. However, we may have $\bar{\mathcal{A}}_{k-1} \mathbf{d}_{k-1} - \bar{\mathbf{b}}_{k-1} \neq 0$, since it is uncertain that the ground truth satisfies the active constraints or not. In this case, from (15)

we have

$$\mathbb{E}[\tilde{\mathbf{d}}_{k-1}] = \gamma_{k-1}^d (\bar{\mathcal{A}}_{k-1} \mathbf{d}_{k-1} - \bar{\mathbf{b}}_{k-1}) \neq 0. \quad (22)$$

A similar statement holds for the state estimation error, and we have

$$\mathbb{E}[\tilde{\mathbf{x}}_k] = \gamma_k^x (\bar{\mathcal{B}}_k \mathbf{x}_k - \bar{\mathbf{c}}_k) \neq 0. \quad (23)$$

These considerations indicate that the projection potentially induces biased estimates, rendering the traditional stability analysis for unbiased estimation invalid. In this context, we will prove that estimation errors of the CARE are practically exponentially stable in mean square, as shown in Section 4.2.

4.1 Performance Analysis

For the analysis of the performance through the projection, we first decompose the state estimation error $\tilde{\mathbf{x}}_k$ into two orthogonal spaces as follows:

$$\tilde{\mathbf{x}}_k = (\mathbf{I} - \gamma_k^x \bar{\mathcal{B}}_k) \tilde{\mathbf{x}}_k + \gamma_k^x \bar{\mathcal{B}}_k \tilde{\mathbf{x}}_k. \quad (24)$$

We will show that the errors in the space $\mathbf{I} - \gamma_k^x \bar{\mathcal{B}}_k$ remain identical after the projection, while the errors in the space $\gamma_k^x \bar{\mathcal{B}}_k$ reduce through the projection, as in Lemma 1.

Lemma 1 *The decomposition of $\tilde{\mathbf{x}}_k$ in the space $\mathbf{I} - \gamma_k^x \bar{\mathcal{B}}_k$ is equal to that of $\tilde{\mathbf{x}}_k^u$, and the decomposition of $\tilde{\mathbf{x}}_k$ in the space $\gamma_k^x \bar{\mathcal{B}}_k$ is equal to that of $\tilde{\mathbf{x}}_k^u$ scaled by α_k , i.e.*

$$(\mathbf{I} - \gamma_k^x \bar{\mathcal{B}}_k) \tilde{\mathbf{x}}_k = (\mathbf{I} - \gamma_k^x \bar{\mathcal{B}}_k) \tilde{\mathbf{x}}_k^u \quad (25)$$

$$\gamma_k^x \bar{\mathcal{B}}_k \tilde{\mathbf{x}}_k = \alpha_k \gamma_k^x \bar{\mathcal{B}}_k \tilde{\mathbf{x}}_k^u, \quad (26)$$

where $\alpha_k = \text{diag}(\alpha_k^1, \dots, \alpha_k^n)$, and

$$\alpha_k^i \triangleq (\gamma_k^x \bar{\mathcal{B}}_k \tilde{\mathbf{x}}_k)(i) ((\gamma_k^x \bar{\mathcal{B}}_k \tilde{\mathbf{x}}_k^u)(i))^\dagger \in [0, 1]$$

for $i = 1, \dots, n$. Similarly, it holds that

$$\begin{aligned} (\mathbf{I} - \gamma_k^d \bar{\mathcal{A}}_k) \tilde{\mathbf{d}}_k &= (\mathbf{I} - \gamma_k^d \bar{\mathcal{A}}_k) \tilde{\mathbf{d}}_k^u \\ \gamma_k^d \bar{\mathcal{A}}_k \tilde{\mathbf{d}}_k &= \kappa_k \gamma_k^d \bar{\mathcal{A}}_k \tilde{\mathbf{d}}_k^u, \end{aligned}$$

where $\kappa_k = \text{diag}(\kappa_k^1, \dots, \kappa_k^n)$, and

$$\kappa_k^i \triangleq (\gamma_k^d \bar{\mathcal{A}}_k \tilde{\mathbf{d}}_k)(i) ((\gamma_k^d \bar{\mathcal{A}}_k \tilde{\mathbf{d}}_k^u)(i))^\dagger \in [0, 1]$$

for $i = 1, \dots, n$.

Proof: The relationship in (25) can be obtained by applying $\bar{\mathbf{B}}_k \hat{\mathbf{x}}_k = \bar{\mathbf{c}}_k$ to

$$\begin{aligned}\tilde{\mathbf{x}}_k &= \mathbf{x}_k - \hat{\mathbf{x}}_k = \mathbf{x}_k - (\hat{\mathbf{x}}_k^u - \gamma_k^x (\bar{\mathbf{B}}_k \hat{\mathbf{x}}_k^u - \bar{\mathbf{c}}_k)) \\ &= \tilde{\mathbf{x}}_k^u + \gamma_k^x (\bar{\mathbf{B}}_k \hat{\mathbf{x}}_k^u - \bar{\mathbf{c}}_k) \\ &= \tilde{\mathbf{x}}_k^u + \gamma_k^x (\bar{\mathbf{B}}_k \hat{\mathbf{x}}_k^u - \bar{\mathbf{B}}_k \hat{\mathbf{x}}_k) \\ &= \tilde{\mathbf{x}}_k^u - \gamma_k^x (\bar{\mathbf{B}}_k \tilde{\mathbf{x}}_k^u - \bar{\mathbf{B}}_k \tilde{\mathbf{x}}_k),\end{aligned}$$

which implies (25). The solution of $\bar{\mathbf{B}}_k \mathbf{x} \leq \bar{\mathbf{c}}_k$ defines a closed convex set \mathcal{C}_k . The point $\hat{\mathbf{x}}_k^u$ is not an element of the convex set. The point $\hat{\mathbf{x}}_k$ has the minimum distance from $\hat{\mathbf{x}}_k^u$ with metric $d(a, b) \triangleq \|a - b\|_{\mathbf{W}_k^x}$ in the convex set \mathcal{C}_k by (19). Since the solution $\hat{\mathbf{x}}_k$ is in the closed set \mathcal{C}_k , and $\gamma_k^x \bar{\mathbf{B}}_k$ is a weighted projection with weight \mathbf{W}_k^x , the relationship (26) holds. The statements for attack estimation errors can be proven by a similar procedure, which is omitted here. ■

With the results from Lemma 1, we can show that the projection reduces the estimation errors and the error covariances, as formulated in Theorem 2.

Theorem 2 CARE reduces the state and attack estimation errors and their error covariances from the unconstrained algorithm, i.e., $\|\tilde{\mathbf{x}}_k\| \leq \|\tilde{\mathbf{x}}_k^u\|$ and $\|\tilde{\mathbf{d}}_k\| \leq \|\tilde{\mathbf{d}}_k^u\|$, $\mathbf{P}_k^x \leq \mathbf{P}_k^{x,u}$ and $\mathbf{P}_k^d \leq \mathbf{P}_k^{d,u}$. Strict inequality holds if $\text{rank}(\bar{\mathbf{B}}_k) \neq 0$, and $\text{rank}(\bar{\mathbf{A}}_k) \neq 0$, respectively.

Proof: The statement for $\|\tilde{\mathbf{x}}_k\| \leq \|\tilde{\mathbf{x}}_k^u\|$ is the direct result of Lemma 1, where strict inequality holds if $\alpha_k^i \neq 0$ for some i . The statement for $\|\tilde{\mathbf{d}}_k\| \leq \|\tilde{\mathbf{d}}_k^u\|$ can be proved by a similar procedure.

To show the rest of the properties, we first identify the equality

$$(\mathbf{I} - \gamma_k^x \bar{\mathbf{B}}_k)^\top \gamma_k^x \bar{\mathbf{B}}_k = 0. \quad (27)$$

Since we have $\bar{\mathbf{B}}_k \gamma_k^x = \mathbf{I}$ by (20), it holds that $\gamma_k^x \bar{\mathbf{B}}_k \gamma_k^x = \gamma_k^x$, and $\bar{\mathbf{B}}_k \gamma_k^x \bar{\mathbf{B}}_k = \bar{\mathbf{B}}_k$, i.e. $\gamma_k^x = \bar{\mathbf{B}}_k^\top$. Then, we have $\bar{\mathbf{B}}_k^\top (\gamma_k^x)^\top \gamma_k^x = \gamma_k^x$, which implies $\tilde{\mathbf{x}}_k^\top (\mathbf{I} - \gamma_k^x \bar{\mathbf{B}}_k)^\top \gamma_k^x \bar{\mathbf{B}}_k \tilde{\mathbf{x}}_k = \tilde{\mathbf{x}}_k^\top (\gamma_k^x \bar{\mathbf{B}}_k - \bar{\mathbf{B}}_k^\top (\gamma_k^x)^\top \gamma_k^x \bar{\mathbf{B}}_k) \tilde{\mathbf{x}}_k = 0$. Notice that (27) holds for $(\tilde{\mathbf{x}}_k^u)^\top (\mathbf{I} - \gamma_k^x \bar{\mathbf{B}}_k)^\top \gamma_k^x \bar{\mathbf{B}}_k \tilde{\mathbf{x}}_k^u = 0$ as well. Inequalities for the covariance can be obtained by taking the trace of the covariance as follows:

$$\begin{aligned}\text{tr}(\mathbf{P}_k^x) &= \text{tr}((\mathbf{I} - \gamma_k^x \bar{\mathbf{B}}_k) \mathbf{P}_k^{x,u} (\mathbf{I} - \gamma_k^x \bar{\mathbf{B}}_k)^\top) \\ &= \text{tr}((\mathbf{I} - \gamma_k^x \bar{\mathbf{B}}_k)^\top (\mathbf{I} - \gamma_k^x \bar{\mathbf{B}}_k) \mathbf{P}_k^{x,u}) \\ &= \text{tr}(\mathbf{I} - \gamma_k^x \bar{\mathbf{B}}_k) \mathbf{P}_k^{x,u} \\ &= \text{tr}(\mathbf{P}_k^{x,u}) - \text{tr}(\gamma_k^x \bar{\mathbf{B}}_k \mathbf{P}_k^{x,u}),\end{aligned}$$

where (27) has been applied. We have the desired result since $\gamma_k^x \bar{\mathbf{B}}_k \mathbf{P}_k^{x,u} = \mathbf{P}_k^{x,u} \bar{\mathbf{B}}_k^\top (\bar{\mathbf{B}}_k \mathbf{P}_k^{x,u} \bar{\mathbf{B}}_k^\top)^{-1} \bar{\mathbf{B}}_k \mathbf{P}_k^{x,u} > 0$. The relation for \mathbf{P}_k^d can be obtained by a similar procedure. ■

The properties in Theorem 2 are desired for accurate estimation as well as attack detection. More specifically, since the false negative rate of a χ^2 attack detector is a function of the estimate $\hat{\boldsymbol{\sigma}}_k$ and the covariance $\boldsymbol{\Sigma}_k$ as in (1), more accurate estimations can reduce the false negative rate under the following assumption.

Assumption 3 In the presence of the attack ($\mathbf{d}_k \neq 0$), the following two conditions hold: (i) $\|\tilde{\mathbf{d}}_k^u\| < \frac{1}{2} \|\mathbf{d}_k\|$, and (ii) the ground truth \mathbf{d}_k satisfies the condition $\mathbf{d}_k^\top (\mathbf{P}_k^{d,u})^{-1} \mathbf{d}_k > \chi_{df}^2(\alpha)$.

Remark 4 Assumption 3 implies that the unconstrained attack estimation error $\tilde{\mathbf{d}}_k^u$ is small with respect to the ground truth \mathbf{d}_k , and the normalized ground truth attack signal is larger than $\chi_{df}^2(\alpha)$; otherwise, it cannot be distinguished from the noise. Notice that Assumption 3 is only considered for smaller false negative rates (Theorem 5), but not for the estimation performance (Theorem 2) and stability analysis in Section 4.2, where we will show the stability of the attack estimation error $\tilde{\mathbf{d}}_k$ (Theorem 8) which renders the stability of $\tilde{\mathbf{d}}_k^u$.

According to (1), we denote the false negative rates of the proposed CARE and the unconstrained algorithm as $F_{neg}(\{\hat{\mathbf{d}}_k\}, \{\mathbf{P}_k^d\})$ and $F_{neg}(\{\hat{\mathbf{d}}_k^u\}, \{\mathbf{P}_k^{d,u}\})$, respectively. The following Theorem 5 demonstrates that the false negative rate of CARE is less or equal to that of the unconstrained algorithm.

Theorem 5 Under Assumption 3, given a set of attack vectors $\{\mathbf{d}_k\}$, the following inequality holds

$$F_{neg}(\{\hat{\mathbf{d}}_k\}, \{\mathbf{P}_k^d\}) \leq F_{neg}(\{\hat{\mathbf{d}}_k^u\}, \{\mathbf{P}_k^{d,u}\}). \quad (28)$$

Proof: To prove (28) is equivalent to showing that the number of false negative test results of CARE is less or equal to that of the unconstrained algorithm

$$\sum_k (\mathbf{1}_k) \leq \sum_k (\mathbf{1}_k^u). \quad (29)$$

If there is no projection ($\gamma_k^d = 0$), it holds that $\hat{\mathbf{d}}_k = \hat{\mathbf{d}}_k^u$ and $\mathbf{P}_k^d = \mathbf{P}_k^{d,u}$. And, if there is no attack ($\mathbf{d}_k = 0$), it holds that $\mathbf{1}_k = \mathbf{1}_k^u = 0$. Therefore, we have

$$\sum_{k \in \mathcal{K}_0} (\mathbf{1}_k) = \sum_{k \in \mathcal{K}_0} (\mathbf{1}_k^u), \quad (30)$$

where $\mathcal{K}_0 \triangleq \{k \mid \gamma_k^d = 0 \text{ or } \mathbf{d}_k = 0\}$. In the rest of the proof, we consider the case for $k \in \mathcal{K} \triangleq \{k \mid \gamma_k^d \neq 0 \text{ and } \mathbf{d}_k \neq 0\}$. Rewriting the normalized test value from CARE by substituting \mathbf{P}_k^d with $(\mathbf{I} - \gamma_k^d \bar{\mathbf{A}}_k) \mathbf{P}_k^{d,u} (\mathbf{I} - \gamma_k^d \bar{\mathbf{A}}_k)^\top$

according to (16), we have the following:

$$\begin{aligned}\hat{\mathbf{d}}_k^\top (\mathbf{P}_k^d)^{-1} \hat{\mathbf{d}}_k &= \hat{\mathbf{d}}_k^\top \left((\mathbf{I} - \gamma_k^d \bar{\mathbf{A}}_k) \mathbf{P}_k^{d,u} (\mathbf{I} - \gamma_k^d \bar{\mathbf{A}}_k)^\top \right)^{-1} \hat{\mathbf{d}}_k \\ &= \left((\mathbf{I} - \gamma_k^d \bar{\mathbf{A}}_k)^{-1} \hat{\mathbf{d}}_k \right)^\top (\mathbf{P}_k^{d,u})^{-1} \left((\mathbf{I} - \gamma_k^d \bar{\mathbf{A}}_k)^{-1} \hat{\mathbf{d}}_k \right) \\ &= (\hat{\mathbf{d}}_k^u + (\mathbf{I} - \gamma_k^d \bar{\mathbf{A}}_k)^{-1} \gamma_k^d \bar{\mathbf{b}}_k)^\top (\mathbf{P}_k^{d,u})^{-1} \\ &\quad \times (\hat{\mathbf{d}}_k^u + (\mathbf{I} - \gamma_k^d \bar{\mathbf{A}}_k)^{-1} \gamma_k^d \bar{\mathbf{b}}_k),\end{aligned}\quad (31)$$

where $(\mathbf{I} - \gamma_k^d \bar{\mathbf{A}}_k)^{-1} \hat{\mathbf{d}}_k = \hat{\mathbf{d}}_k^u + (\mathbf{I} - \gamma_k^d \bar{\mathbf{A}}_k)^{-1} \gamma_k^d \bar{\mathbf{b}}_k$ has been applied. Now we expand and rearrange (31), resulting in the following:

$$\begin{aligned}\hat{\mathbf{d}}_k^\top (\mathbf{P}_k^d)^{-1} \hat{\mathbf{d}}_k &= (\hat{\mathbf{d}}_k^u)^\top (\mathbf{P}_k^{d,u})^{-1} \hat{\mathbf{d}}_k^u \\ &+ \left((\mathbf{I} - \gamma_k^d \bar{\mathbf{A}}_k)^{-1} \gamma_k^d \bar{\mathbf{b}}_k \right)^\top (\mathbf{P}_k^{d,u})^{-1} \left((\mathbf{I} - \gamma_k^d \bar{\mathbf{A}}_k)^{-1} \gamma_k^d \bar{\mathbf{b}}_k \right) \\ &+ 2(\hat{\mathbf{d}}_k^u)^\top (\mathbf{P}_k^{d,u})^{-1} \left((\mathbf{I} - \gamma_k^d \bar{\mathbf{A}}_k)^{-1} \gamma_k^d \bar{\mathbf{b}}_k \right) \\ &= (\hat{\mathbf{d}}_k^u)^\top (\mathbf{P}_k^{d,u})^{-1} \hat{\mathbf{d}}_k^u \\ &+ (\gamma_k^d \bar{\mathbf{b}}_k)^\top \left((\mathbf{I} - \gamma_k^d \bar{\mathbf{A}}_k) \mathbf{P}_k^{d,u} (\mathbf{I} - \gamma_k^d \bar{\mathbf{A}}_k)^\top \right)^{-1} \gamma_k^d \bar{\mathbf{b}}_k \\ &+ 2(\hat{\mathbf{d}}_k^u)^\top \left((\mathbf{I} - \gamma_k^d \bar{\mathbf{A}}_k) \mathbf{P}_k^{d,u} \right)^{-1} \gamma_k^d \bar{\mathbf{b}}_k.\end{aligned}\quad (32)$$

Applying (16) and (17) to (32), we have

$$\begin{aligned}\hat{\mathbf{d}}_k^\top (\mathbf{P}_k^d)^{-1} \hat{\mathbf{d}}_k &= (\hat{\mathbf{d}}_k^u)^\top (\mathbf{P}_k^{d,u})^{-1} \hat{\mathbf{d}}_k^u \\ &+ \underbrace{(\gamma_k^d \bar{\mathbf{b}}_k)^\top (\mathbf{P}_k^d)^{-1} \gamma_k^d \bar{\mathbf{b}}_k + 2(\hat{\mathbf{d}}_k^u)^\top (\mathbf{P}_k^d)^{-1} \gamma_k^d \bar{\mathbf{b}}_k}_{\triangleq \text{residue (res.)}}.\end{aligned}\quad (33)$$

Since $\hat{\mathbf{d}}_k$ satisfies the input active constraint, we can substitute $\bar{\mathbf{b}}_k$ with $\bar{\mathbf{A}}_k \hat{\mathbf{d}}_k$. Then the residue defined in (33) can be written as follows:

$$\begin{aligned}\text{res.} &= (\gamma_k^d \bar{\mathbf{A}}_k \hat{\mathbf{d}}_k)^\top (\mathbf{P}_k^d)^{-1} \gamma_k^d \bar{\mathbf{A}}_k \hat{\mathbf{d}}_k \\ &+ 2(\hat{\mathbf{d}}_k^u)^\top (\mathbf{P}_k^d)^{-1} \gamma_k^d \bar{\mathbf{A}}_k \hat{\mathbf{d}}_k.\end{aligned}\quad (34)$$

Expanding and rearranging (34), we have the following:

$$\text{res.} = 2\tilde{\mathbf{d}}_k^\top \mathbf{P}'_k \mathbf{d}_k - 2\tilde{\mathbf{d}}_k^\top \mathbf{P}'_k \mathbf{d}_k - 2(\tilde{\mathbf{d}}_k^u)^\top \mathbf{P}'_k \mathbf{d}_k \quad (35)$$

$$+ 2\tilde{\mathbf{d}}_k^\top \mathbf{P}'_k \tilde{\mathbf{d}}_k + \|\gamma_k^d \bar{\mathbf{A}}_k\|^2 \tilde{\mathbf{d}}_k^\top (\mathbf{P}_k^d)^{-1} \tilde{\mathbf{d}}_k \quad (36)$$

$$+ \|\gamma_k^d \bar{\mathbf{A}}_k\|^2 \tilde{\mathbf{d}}_k^\top (\mathbf{P}_k^d)^{-1} \mathbf{d}_k - 2\|\gamma_k^d \bar{\mathbf{A}}_k\|^2 \tilde{\mathbf{d}}_k^\top (\mathbf{P}_k^d)^{-1} \tilde{\mathbf{d}}_k, \quad (37)$$

where $\mathbf{P}'_k \triangleq (\gamma_k^d \bar{\mathbf{A}}_k)^\top (\mathbf{P}_k^d)^{-1} > 0$. Using the result $\|\tilde{\mathbf{d}}_k\| < \|\tilde{\mathbf{d}}_k^u\|$ from Theorem 2 and the first inequality in Assumption 3, we obtain $\|\tilde{\mathbf{d}}\| < \|\tilde{\mathbf{d}}^u\| < \frac{1}{2}\|\tilde{\mathbf{d}}\|$. Then we have $\text{res.} > 0$, since (35) to (37) are positive, respectively. Therefore, from (33), we have

$$(\hat{\mathbf{d}}_k^u)^\top (\mathbf{P}_k^{d,u})^{-1} \hat{\mathbf{d}}_k^u < \hat{\mathbf{d}}_k^\top (\mathbf{P}_k^d)^{-1} \hat{\mathbf{d}}_k. \quad (38)$$

Considering the condition in (38), we can divide the set

$\mathcal{K} = \cup_{i=1}^3 \mathcal{K}_i$ into three partitions as follows:

$$\mathcal{K}_1 \triangleq \{k \mid (\hat{\mathbf{d}}_k^u)^\top (\mathbf{P}_k^{d,u})^{-1} \hat{\mathbf{d}}_k^u < \hat{\mathbf{d}}_k^\top (\mathbf{P}_k^d)^{-1} \hat{\mathbf{d}}_k \leq \chi_{df}^2(\alpha)\}$$

$$\mathcal{K}_2 \triangleq \{k \mid \chi_{df}^2(\alpha) < (\hat{\mathbf{d}}_k^u)^\top (\mathbf{P}_k^{d,u})^{-1} \hat{\mathbf{d}}_k^u < \hat{\mathbf{d}}_k^\top (\mathbf{P}_k^d)^{-1} \hat{\mathbf{d}}_k\}$$

$$\mathcal{K}_3 \triangleq \{k \mid (\hat{\mathbf{d}}_k^u)^\top (\mathbf{P}_k^{d,u})^{-1} \hat{\mathbf{d}}_k^u \leq \chi_{df}^2(\alpha) < \hat{\mathbf{d}}_k^\top (\mathbf{P}_k^d)^{-1} \hat{\mathbf{d}}_k\}.$$

According to (2), we have

$$\sum_{k \in \mathcal{K}_i} (\mathbf{1}_k) = \sum_{k \in \mathcal{K}_i} (\mathbf{1}_k^u) \text{ for } i = 1, 2 \text{ and} \quad (39)$$

$$\sum_{k \in \mathcal{K}_3} (\mathbf{1}_k) < \sum_{k \in \mathcal{K}_3} (\mathbf{1}_k^u). \quad (40)$$

Therefore, from (30), (39) and (40) we conclude that (29) holds, which completes the proof. \blacksquare

4.2 Stability Analysis

Although the projection reduces the estimation errors and their error covariances as shown in Theorem 2, it trades the unbiased estimation off according to (22) and (23). In the absence of the projection, Algorithm 1 reduces to the algorithm in Yong et al. (2016), which is an unbiased estimation, while the traditional stability analysis for unbiased estimation becomes invalid after the projection is applied.

To prove the recursive stability of the biased estimation, it is essential to construct a recursive relation between the current estimation error $\tilde{\mathbf{x}}_k$ and the previous estimation error $\tilde{\mathbf{x}}_{k-1}$. However, the construction is not straightforward comparing to that in filtering with equality constraints (Simon and Chia, 2002; Yong et al., 2015b) or filtering without constraints (Anderson and Moore, 1981; Yong et al., 2016). Especially, it is difficult to find the exact recursive relation between $\tilde{\mathbf{x}}_k$ and $\tilde{\mathbf{x}}_k^u$, since $\tilde{\mathbf{x}}_k$ is also a function of $\hat{\mathbf{x}}_k^u$, i.e. $\tilde{\mathbf{x}}_k = \tilde{\mathbf{x}}_k^u - \gamma_k^x (\bar{\mathbf{B}}_k \hat{\mathbf{x}}_k^u - \bar{\mathbf{c}}_k)$. Then, we have $\tilde{\mathbf{x}}_k \neq (\mathbf{I} - \gamma_k^x \bar{\mathbf{B}}_k) \tilde{\mathbf{x}}_k^u$ because of the inequality $\bar{\mathbf{B}}_k \mathbf{x}_k \leq \bar{\mathbf{c}}_k$. To address this issue, we decompose the estimation error $\tilde{\mathbf{x}}_k$ into two orthogonal spaces as in (24). By Lemma 1, (24) becomes

$$\tilde{\mathbf{x}}_k = \mathbf{\Gamma}_k \tilde{\mathbf{x}}_k^u,$$

where $\mathbf{\Gamma}_k \triangleq (\mathbf{I} - \gamma_k^x \bar{\mathbf{B}}_k) + \alpha_k \gamma_k^x \bar{\mathbf{B}}_k$. Note that α_k is an unknown matrix and thus cannot be used for the algorithm. We use it only for analytical purposes.

Now under the following assumptions, we present the stability analysis of the proposed Algorithm 1.

Assumption 6 We have $\text{rank}(\bar{\mathbf{B}}_k) < n \forall k$. There exist $\bar{a}, \bar{c}_y, \bar{g}, \bar{m}, \underline{q}, \underline{\beta}, \bar{\beta} > 0$, such that the following holds for

all $k \geq 0$:

$$\begin{aligned} \|\mathbf{A}_k\| &\leq \bar{a}, & \|\mathbf{C}_k\| &\leq \bar{c}_y, & \|\mathbf{G}_k\| &\leq \bar{g}, \\ \|\mathbf{M}_k\| &\leq \bar{m}, & \mathbf{Q}_k &\geq \underline{q}\mathbf{I}. \end{aligned}$$

Remark 7 In Assumption 6, it is assumed that $\text{rank}(\mathbf{B}_k) < n \forall k$, i.e., the number of the state constraints are less than the number of state variables. The rest of Assumption 6 is widely used in the literature on extended Kalman filtering (Kluge et al., 2010) and nonlinear input and state estimation (Kim et al., 2017).

Theorem 8 Consider Assumption 6 and assume that there exist non-negative constants \underline{p} and \bar{p} such that $\underline{p}\mathbf{I} \leq \mathbf{P}_k^{x,u} \leq \bar{p}\mathbf{I}$ holds for all k . Then the estimation errors $\tilde{\mathbf{x}}_k$ and $\tilde{\mathbf{d}}_k$ are practically exponentially stable in mean square, i.e., there exist constants $a_x, a_d, b_x, b_d, c_x, c_d$ such that for all k

$$\begin{aligned} \mathbb{E}[\|\tilde{\mathbf{x}}_k\|^2] &\leq a_x e^{-b_x k} \mathbb{E}[\|\tilde{\mathbf{x}}_0\|^2] + c_x \\ \mathbb{E}[\|\tilde{\mathbf{d}}_k\|^2] &\leq a_d e^{-b_d k} \mathbb{E}[\|\tilde{\mathbf{d}}_0\|^2] + c_d. \end{aligned}$$

Proof: See Appendix A.

Theorem 8 holds under the assumption of boundedness of $\mathbf{P}_k^{x,u}$. One of the sufficient conditions is the uniform detectability of the transformed system as shown in the following Theorem 9.

Theorem 9 If the pair $(\mathbf{C}_k, \tilde{\mathbf{A}}_{k-1})$ is uniformly detectable, then there exist non-negative constants \underline{p} and \bar{p} such that $\underline{p}\mathbf{I} \leq \mathbf{P}_k^{x,u} \leq \bar{p}\mathbf{I}$ for all k , where $\tilde{\mathbf{A}}_{k-1} \triangleq (\mathbf{I} - \mathbf{G}_{k-1}\mathbf{M}_k(\mathbf{C}_k\mathbf{G}_{k-1}\mathbf{M}_k)^{-1}\mathbf{C}_k)\bar{\mathbf{A}}_{k-1}\bar{\mathbf{\Gamma}}_{k-1}$ and $\bar{\mathbf{A}}_{k-1} \triangleq (\mathbf{I} - \mathbf{G}_{k-1}\mathbf{M}_k\mathbf{C}_k)\mathbf{A}_{k-1}$.

Proof: The unconstrained state estimation error can be found by

$$\begin{aligned} \tilde{\mathbf{x}}_k^u &= (\mathbf{I} - \mathbf{L}_k\mathbf{C}_k)\bar{\mathbf{A}}_{k-1}\tilde{\mathbf{x}}_{k-1} \\ &\quad + (\mathbf{I} - \mathbf{L}_k\mathbf{C}_k)\tilde{\mathbf{w}}_{k-1} + \bar{\mathbf{L}}_k\mathbf{v}_k, \end{aligned} \quad (41)$$

where $\tilde{\mathbf{w}}_{k-1} \triangleq (\mathbf{I} - \mathbf{G}_{k-1}\mathbf{M}_k\mathbf{C}_k)\mathbf{w}_{k-1}$, and $\bar{\mathbf{L}}_k \triangleq \mathbf{L}_k\mathbf{C}_k\mathbf{G}_{k-1}\mathbf{M}_k - \mathbf{L}_k - \mathbf{G}_{k-1}\mathbf{M}_k$. Therefore, the update law of unconstrained covariance is calculated from (41) and (21) as follows:

$$\begin{aligned} \mathbf{P}_k^{x,u} &= (\mathbf{I} - \mathbf{L}_k\mathbf{C}_k)\bar{\mathbf{A}}_{k-1}\bar{\mathbf{\Gamma}}_{k-1}\mathbf{P}_{k-1}^{x,u}\bar{\mathbf{\Gamma}}_{k-1}^\top \\ &\quad \times \bar{\mathbf{A}}_{k-1}^\top(\mathbf{I} - \mathbf{L}_k\mathbf{C}_k)^\top + \bar{\mathbf{L}}_k\mathbf{R}_k\bar{\mathbf{L}}_k^\top \\ &\quad + (\mathbf{I} - \mathbf{L}_k\mathbf{C}_k)\bar{\mathbf{Q}}_{k-1}(\mathbf{I} - \mathbf{L}_k\mathbf{C}_k)^\top, \end{aligned} \quad (42)$$

where $\bar{\mathbf{Q}}_{k-1} \triangleq \mathbb{E}[\tilde{\mathbf{w}}_{k-1}(\tilde{\mathbf{w}}_{k-1})^\top]$. The covariance update law (42) is identical to the covariance update law of the Kalman filtering solution of the transformed system

$$\begin{aligned} \mathbf{x}_k &= \bar{\mathbf{A}}_{k-1}\bar{\mathbf{\Gamma}}_{k-1}\mathbf{x}_{k-1} + \hat{\mathbf{w}}_{k-1} \\ \mathbf{y}_k &= \mathbf{C}_k\mathbf{x}_k + \mathbf{v}_k, \end{aligned} \quad (43)$$

where $\hat{\mathbf{w}}_{k-1} \triangleq -\mathbf{G}_{k-1}\mathbf{M}_k\mathbf{C}_k\mathbf{w}_{k-1} - \mathbf{G}_{k-1}\mathbf{M}_k\mathbf{v}_k + \mathbf{w}_{k-1}$. However, in the transformed system, the process noise and measurement noise are correlated, i.e., $\mathbb{E}[\hat{\mathbf{w}}_{k-1}\mathbf{v}_k^\top] = -\mathbf{G}_{k-1}\mathbf{M}_k\mathbf{R}_k \neq 0$. To decouple the noises, we add a zero term $\mathbf{Z}_k(\mathbf{y}_k - \mathbf{C}_k(\bar{\mathbf{A}}_{k-1}\bar{\mathbf{\Gamma}}_{k-1}\mathbf{x}_k + \hat{\mathbf{w}}_{k-1}) - \mathbf{v}_k)$ to the state equation in (43), and obtain the following:

$$\mathbf{x}_k = \tilde{\mathbf{A}}_{k-1}\mathbf{x}_{k-1} + \tilde{\mathbf{u}}_{k-1} + \tilde{\mathbf{w}}_{k-1},$$

where $\tilde{\mathbf{A}}_{k-1} \triangleq (\mathbf{I} - \mathbf{Z}_k\mathbf{C}_k)\bar{\mathbf{A}}_{k-1}\bar{\mathbf{\Gamma}}_{k-1}$, $\tilde{\mathbf{u}}_{k-1} \triangleq \mathbf{Z}_k\mathbf{y}_k$ is the known input, and $\tilde{\mathbf{w}}_{k-1} \triangleq (\mathbf{I} - \mathbf{Z}_k\mathbf{C}_k)\hat{\mathbf{w}}_{k-1} - \mathbf{Z}_k\mathbf{v}_k$ is the new process noise. The new process noise and the measurement noise could be decoupled by choosing the gain \mathbf{Z}_k such that $\mathbb{E}[\tilde{\mathbf{w}}_{k-1}\mathbf{v}_k^\top] = 0$. The solution can be found by $\mathbf{Z}_k = \mathbf{G}_{k-1}\mathbf{M}_k(\mathbf{C}_k\mathbf{G}_{k-1}\mathbf{M}_k)^{-1}$. Then, the system (43) becomes

$$\begin{aligned} \mathbf{x}_{k+1} &= \tilde{\mathbf{A}}_k\mathbf{x}_k + \tilde{\mathbf{u}}_k + \tilde{\mathbf{w}}_k \\ \mathbf{y}_k &= \mathbf{C}_k\mathbf{x}_k + \mathbf{v}_k. \end{aligned}$$

Since the pair $(\mathbf{C}_k, \tilde{\mathbf{A}}_k)$ is uniformly detectable, by Theorem 5.2 in Anderson and Moore (1981), the statement holds. \blacksquare

5 Illustrative Example

In this example, we test Algorithm 1 on a vehicle model with input and state constraints and compare the estimation accuracy and the detection performance with an unconstrained algorithm.

5.1 Experimental Setup

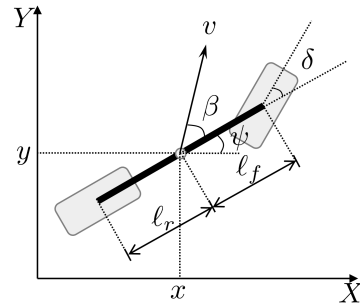


Fig. 2. Kinematic Bicycle Model.

We consider a kinematic bicycle model (Fig. 2) in Kong et al. (2015); Rajamani (2011). The nonlinear

Table 1
Performance comparison.

	$\sum_k \ \tilde{\mathbf{x}}_k\ $	$\sum_k \ \tilde{\mathbf{d}}_k\ $	$\sum_k \ \text{tr}(\mathbf{P}_k^x)\ $	$\sum_k \ \text{tr}(\mathbf{P}_k^d)\ $
CARE	88.928	672.914	0.455	27.351*
ISE	123.623	1041.837	0.613	40.577*

* The summation ranges from $k = 100$ to $k = 1000$ due to the large initialization (10^4 -scale), as shown in Fig. 4.

continuous-time model is given as

$$\begin{aligned}\dot{x} &= v \cos(\psi + \beta) \\ \dot{y} &= v \sin(\psi + \beta) \\ \dot{\psi} &= \frac{v}{l_r} \sin(\beta) \\ \dot{v} &= a \\ \beta &= \arctan\left(\frac{l_r}{l_f + l_r} \tan(\delta)\right),\end{aligned}$$

where x and y are the coordinates of the center of mass, v is the velocity of the center of mass, β is the angle of the velocity v with respect to the longitudinal axis of the vehicle, a is the acceleration, ψ is the heading angle of the vehicle, δ is the steering angle of the front wheel, and l_f and l_r represent the distance from the center of mass of the vehicle to the front and rear axles, respectively.

Since the proposed algorithm is for linear discrete-time systems, we perform the linearization and discretization as in Law et al. (2018) with sampling time $T_s = 0.01s$. We rewrite the system in the form of (3), where $\mathbf{x}_k = [x_k, y_k, \psi_k, v_k]^\top$ is the state vector, $\mathbf{u}_k = [\beta_k^u, a_k^u]^\top = \left[\arctan\left(\frac{l_r}{l_f + l_r} \tan(\delta_k^u)\right), a_k^u\right]^\top$ is the input vector, and $\mathbf{d}_k = [\beta_k^d, a_k^d]^\top = \left[\arctan\left(\frac{l_r}{l_f + l_r} \tan(\delta_k^d)\right), a_k^d\right]^\top$ is the attack input vector. We consider the scenario that attack input is injected into the input, i.e. $\mathbf{G}_k = \mathbf{B}_k$. The system matrices are given as follows:

$$\mathbf{A}_k = \begin{bmatrix} 1 & 0 & 0 & T_s \\ 0 & 1 & v_k T_s & 0 \\ 0 & 0 & 1 & 0 \\ 0 & 0 & 0 & 1 \end{bmatrix}, \quad \mathbf{B}_k = \mathbf{G}_k = \begin{bmatrix} 0 & 0 \\ v_k T_s & 0 \\ \frac{v_k T_s}{l_r} & 0 \\ 0 & T_s \end{bmatrix}, \quad \mathbf{C}_k = \mathbf{I}.$$

The noise covariances \mathbf{Q}_k and \mathbf{R}_k are considered as diagonal matrices with $\text{diag}(\mathbf{Q}_k) = [0.1, 0.1, 0.001, 0.0001]$ and $\text{diag}(\mathbf{R}_k) = [0.01, 0.01, 0.001, 0.00001]$.

The vehicle is assumed to have state constraints on the location $0 \leq x_k \leq 20$, $0 \leq y_k \leq 5$ and the velocity $0 \leq v_k \leq 22$, and input constraints on the steering angle $|\delta| \leq 1.0472$ and the acceleration $|a| \leq 3.5$.

The unknown attack signals are

$$\begin{aligned}\delta_k^d &= \begin{cases} 0, & 0 \leq k < 100 \\ 1.1 \sin(0.05k), & 100 \leq k < 1000 \end{cases} \\ a_k^d &= \begin{cases} 0 & 0 \leq k < 100 \\ 3.5, & 100n \leq k < 100(n+1) \\ -3.5, & 100(n+1) \leq k < 100(n+2) \end{cases},\end{aligned}$$

where $n = 1, 2, \dots, 5$.

The constraints on the vehicle can be formulated by inequality constraints as in (4):

$$\underbrace{\begin{bmatrix} 1 & 0 \\ -1 & 0 \\ 0 & 1 \\ 0 & -1 \end{bmatrix}}_{\mathbf{A}_{k-1}} \underbrace{\begin{bmatrix} \delta_{k-1}^d \\ a_{k-1}^d \end{bmatrix}}_{\mathbf{b}_{k-1}} \leq \underbrace{\begin{bmatrix} 1.0472 - \delta_{k-1}^u \\ 1.0472 + \delta_{k-1}^u \\ 3.5 - a_{k-1}^u \\ 3.5 + a_{k-1}^u \end{bmatrix}}_{\mathbf{b}_{k-1}}$$

$$\underbrace{\begin{bmatrix} 1 & 0 & 0 & 0 \\ -1 & 0 & 0 & 0 \\ 0 & 1 & 0 & 0 \\ 0 & -1 & 0 & 0 \\ 0 & 0 & 0 & 1 \\ 0 & 0 & 0 & -1 \end{bmatrix}}_{\mathbf{B}_k} \underbrace{\begin{bmatrix} x_k \\ y_k \\ \psi_k \\ v_k \end{bmatrix}}_{\mathbf{c}_k} \leq \underbrace{\begin{bmatrix} 20 \\ 0 \\ 5 \\ 0 \\ 22 \\ 0 \end{bmatrix}}_{\mathbf{c}_k}.$$

To reduce the effect of instantaneous noises, the cumulative sum algorithm (CUSUM) is adopted, which is widely used in attack detection research (Page, 1954; Barnard, 1959; Lai, 1995). The χ^2 test in Section 2.2 is utilized in a cumulative form. The χ^2 CUSUM detector is characterized by the detector state $S_k \in \mathbb{R}_+$:

$$S_k = \phi S_{k-1} + \hat{\mathbf{d}}_k^\top \mathbf{P}_k^{-1} \hat{\mathbf{d}}_k, \quad S_0 = 0, \quad (44)$$

where $0 < \phi < 1$ is the pre-determined forgetting rate. At each time k , the CUSUM detector (44) is used to update the detector state S_k and detect the attack. In particular, we conclude that the attack is presented if

$$S_k > \sum_{i=0}^{\infty} \phi^i \chi_{df}^2(\alpha) = \frac{\chi_{df}^2(\alpha)}{1 - \phi}. \quad (45)$$

All values are in standard SI units: m (meter) for l_f, l_r, x_k , and y_k ; rad for $\delta_k^u, \delta_k^d, \beta_k^u, \beta_k^d$, and ψ_k ; m/s for v_k ; m/s^2 for a_k^u and a_k^d .

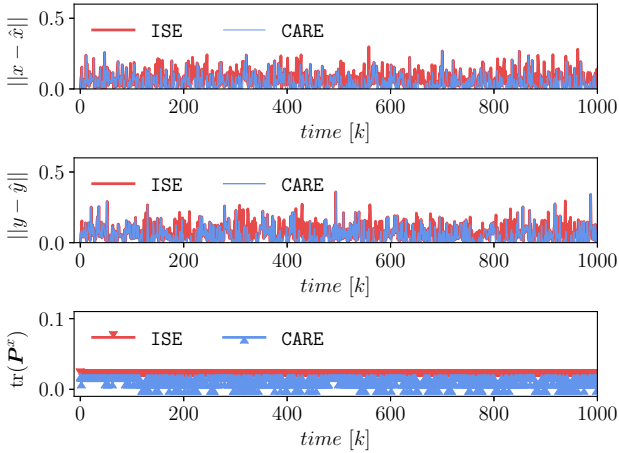


Fig. 3. Estimation errors of constrained states and traces of the state error covariance.

5.2 Results

We show a comparison of the proposed algorithm (**CARE**) and the unified linear input and state estimator (**ISE**) introduced in Yong et al. (2016). Figure 3 shows the estimation errors of the constrained states (x_k and y_k) and the traces of the state error covariances, and Fig. 4 shows the unknown attack signals and their estimates and traces of the attack estimation error covariances. As expected, **CARE** produces smaller state estimation error and lower covariance. When the attack happens after $k = 100$, the estimates obtained by **CARE** are closer to the true values and have lower error covariances (cf. Table 1).

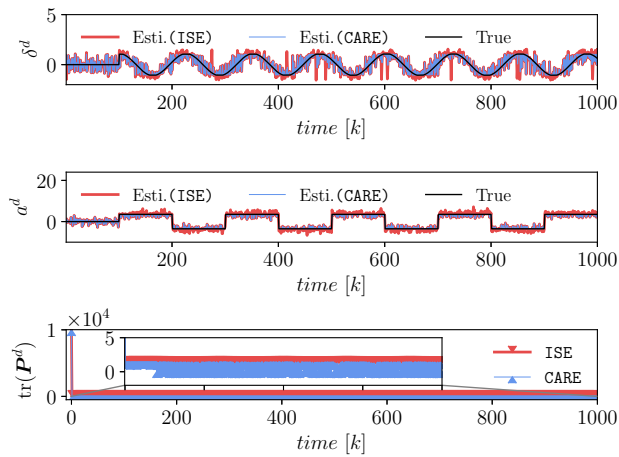


Fig. 4. Attack signal estimation and traces of error covariance of the attack signals.

The estimates are used to calculate the detector state S_k in (44). The statistical significance of the attack is

tested using the CUSUM detector. The threshold is calculated by $\chi_{df}^2/(1-\phi)$ in (45) with the significance level $\alpha = 0.01$ and the forgetting rate $\phi = 0.15$. The detector states and the threshold are plotted in \log -scale (Fig. 5). When the attack is present, **CARE** can detect the attack by producing high detector state values above the threshold, while the detector state values from **ISE** are oscillating around the threshold, suffering from a high false negative rate of 66.44%.

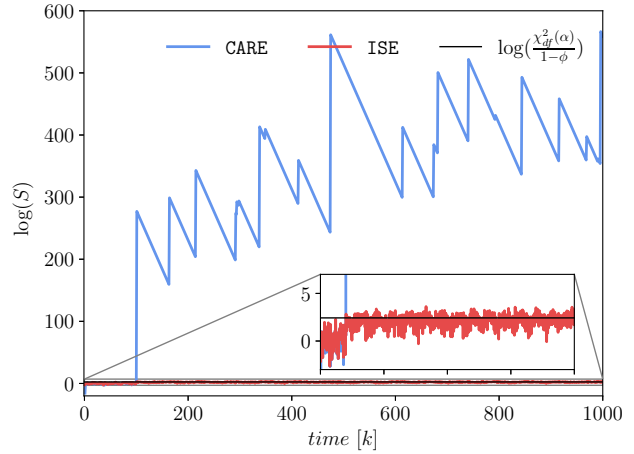


Fig. 5. Attack detection.

6 Conclusion

In this paper, we presented a constrained attack-resilient estimation algorithm (**CARE**) of linear stochastic cyber-physical systems. The proposed algorithm utilizes physical constraints and operational limitations via projection to improve estimation accuracy and detection performance. In particular, **CARE** first provides minimum-variance unbiased estimates, and then these estimates are projected onto the constrained space. We formally proved that estimation errors and their covariances from **CARE** are less than those from unconstrained algorithms, and showed that **CARE** has improved false negative rate in attack detection. Moreover, we proved that the estimation errors of the proposed estimation algorithm are practically exponentially stable. A simulation of attacks on a vehicle demonstrates the effectiveness of the proposed algorithm and reveals better attack-resilient properties compared to an existing algorithm.

Acknowledgements

This work has been supported by the National Science Foundation (ECCS-1739732 and CMMI-1663460).

A Proof of Theorem 8

Consider the Lyapunov function

$$V_k = (\tilde{\mathbf{x}}_k^u)^\top (\mathbf{P}_k^{x,u})^{-1} (\tilde{\mathbf{x}}_k^u).$$

After substituting (41) into the Lyapunov function, we obtain

$$\begin{aligned} V_k &= (\tilde{\mathbf{x}}_{k-1}^u)^\top \mathbf{\Gamma}_{k-1}^\top \bar{\mathbf{A}}_{k-1}^\top (\mathbf{I} - \mathbf{L}_k \mathbf{C}_k)^\top (\mathbf{P}_k^{x,u})^{-1} \\ &\quad \times (\mathbf{I} - \mathbf{L}_k \mathbf{C}_k) \bar{\mathbf{A}}_{k-1} \mathbf{\Gamma}_{k-1} \tilde{\mathbf{x}}_{k-1}^u \\ &\quad + 2(\tilde{\mathbf{x}}_{k-1}^u)^\top \mathbf{\Gamma}_{k-1}^\top \bar{\mathbf{A}}_{k-1}^\top (\mathbf{I} - \mathbf{L}_k \mathbf{C}_k)^\top \\ &\quad \times (\mathbf{P}_k^{x,u})^{-1} (\mathbf{I} - \mathbf{L}_k \mathbf{C}_k) \bar{\mathbf{w}}_{k-1} \\ &\quad + 2(\tilde{\mathbf{x}}_{k-1}^u)^\top \mathbf{\Gamma}_{k-1}^\top \bar{\mathbf{A}}_{k-1}^\top (\mathbf{I} - \mathbf{L}_k \mathbf{C}_k)^\top (\mathbf{P}_k^{x,u})^{-1} \bar{\mathbf{L}}_k \mathbf{v}_k \\ &\quad + \bar{\mathbf{w}}_{k-1}^\top (\mathbf{I} - \mathbf{L}_k \mathbf{C}_k)^\top (\mathbf{P}_k^{x,u})^{-1} (\mathbf{I} - \mathbf{L}_k \mathbf{C}_k) \bar{\mathbf{w}}_{k-1} \\ &\quad + 2\mathbf{w}_{k-1}^\top (\mathbf{I} - \mathbf{L}_k \mathbf{C}_k)^\top (\mathbf{P}_k^{x,u})^{-1} \bar{\mathbf{L}}_k \mathbf{v}_k \\ &\quad + \mathbf{v}_k^\top \bar{\mathbf{L}}_k (\mathbf{P}_k^{x,u})^{-1} \bar{\mathbf{L}}_k \mathbf{v}_k. \end{aligned} \quad (\text{A.1})$$

By the uncorrelatedness property (Papoulis and Pillai, 2002) of \mathbf{w}_{k-1} , \mathbf{v}_k and $\tilde{\mathbf{x}}_{k-1}^u$, the Lyapunov function (A.1) becomes

$$\begin{aligned} \mathbb{E}[V_k] &= \mathbb{E}[(\tilde{\mathbf{x}}_{k-1}^u)^\top \mathbf{\Gamma}_{k-1}^\top \bar{\mathbf{A}}_{k-1}^\top (\mathbf{I} - \mathbf{L}_k \mathbf{C}_k)^\top (\mathbf{P}_k^{x,u})^{-1} \\ &\quad \times \bar{\mathbf{A}}_{k-1} (\mathbf{I} - \mathbf{L}_k \mathbf{C}_k) \mathbf{\Gamma}_{k-1} (\tilde{\mathbf{x}}_{k-1}^u)] \\ &\quad + \mathbb{E}[\bar{\mathbf{w}}_{k-1}^\top (\mathbf{I} - \mathbf{L}_k \mathbf{C}_k)^\top (\mathbf{P}_k^{x,u})^{-1} (\mathbf{I} - \mathbf{L}_k \mathbf{C}_k) \bar{\mathbf{w}}_{k-1}] \\ &\quad + \mathbb{E}[\mathbf{v}_k^\top \bar{\mathbf{L}}_k (\mathbf{P}_k^{x,u})^{-1} \bar{\mathbf{L}}_k \mathbf{v}_k]. \end{aligned} \quad (\text{A.2})$$

The following statements are formulated to deal with each term in (A.2).

Claim 10 *There exists a constant $\delta \triangleq (\frac{q'}{\bar{a}^2 \bar{p}} + 1)^{-1} \in (0, 1)$, such that $\mathbf{\Gamma}_{k-1}^\top \bar{\mathbf{A}}_{k-1}^\top (\mathbf{I} - \mathbf{L}_k \mathbf{C}_k)^\top (\mathbf{P}_k^{x,u})^{-1} (\mathbf{I} - \mathbf{L}_k \mathbf{C}_k) \bar{\mathbf{A}}_{k-1} \mathbf{\Gamma}_{k-1} < \delta (\mathbf{P}_k^{x,u})^{-1}$.*

Proof: *Since $\text{rank}(\mathbf{B}_k) < n \forall k$, it holds that $\text{rank}(\bar{\mathbf{B}}_k) < n \forall k$ and thus $\bar{\mathbf{\Gamma}} \neq 0$. Therefore, $\|\bar{\mathbf{\Gamma}}_{k-1}\| = 1$ because $\gamma_{k-1}^x \bar{\mathbf{B}}_{k-1}$ is a projection matrix. From Assumption 6 and Theorem 9, we have*

$$\bar{\mathbf{Q}}_{k-1} \geq \underline{q}' \mathbf{I}, \quad \mathbf{P}_{k-1}^x \leq \bar{p} \mathbf{I}.$$

Since $\|\bar{\mathbf{A}}_{k-1}\|$ is upper bounded by $\bar{a}' \triangleq \bar{a}(1 + \bar{g}\bar{m}\bar{c}_y)$, we can have $\bar{\mathbf{A}}_{k-1} \bar{\mathbf{A}}_{k-1}^\top \leq \bar{a}'^2 \mathbf{I}$. Then we have

$$\begin{aligned} \bar{\mathbf{Q}}_{k-1} &\geq \underline{q}' \frac{\bar{\mathbf{A}}_{k-1} \bar{\mathbf{A}}_{k-1}^\top}{\bar{a}'^2} \geq \frac{\underline{q}'}{\bar{a}'^2} \bar{\mathbf{A}}_{k-1} \bar{\mathbf{\Gamma}}_{k-1} \bar{\mathbf{\Gamma}}_{k-1}^\top \bar{\mathbf{A}}_{k-1}^\top \\ &\geq \frac{\underline{q}'}{\bar{a}'^2 \bar{p}} \bar{\mathbf{A}}_{k-1} \bar{\mathbf{\Gamma}}_{k-1} \mathbf{P}_{k-1}^{x,u} \bar{\mathbf{\Gamma}}_{k-1}^\top \bar{\mathbf{A}}_{k-1}^\top. \end{aligned} \quad (\text{A.3})$$

Substitution of (A.3) into (42) yields

$$\begin{aligned} \mathbf{P}_k^{x,u} - (1 + \frac{\underline{q}'}{\bar{a}'^2 \bar{p}}) (\mathbf{I} - \mathbf{L}_k \mathbf{C}_k) \bar{\mathbf{A}}_{k-1} \bar{\mathbf{\Gamma}}_{k-1} \mathbf{P}_{k-1}^{x,u} \bar{\mathbf{\Gamma}}_{k-1}^\top \bar{\mathbf{A}}_{k-1}^\top \\ \times (\mathbf{I} - \mathbf{L}_k \mathbf{C}_k)^\top > 0, \end{aligned} \quad (\text{A.4})$$

where the inequality holds because $\mathbf{R}_k > 0$. As $(1 + \frac{\underline{q}'}{\bar{a}'^2 \bar{p}}) \mathbf{P}_{k-1}^{x,u} > 0$, the inverse of the left hand side of (A.4) exists and is symmetric positive definite. By the matrix inversion lemma (Tylavsky and Sohie, 1986), it follows that

$$\begin{aligned} (1 + \frac{\underline{q}'}{\bar{a}'^2 \bar{p}})^{-1} (\mathbf{P}_{k-1}^{x,u})^{-1} - \bar{\mathbf{\Gamma}}_{k-1}^\top \bar{\mathbf{A}}_{k-1}^\top (\mathbf{I} - \mathbf{L}_k \mathbf{C}_k)^\top \\ \times (\mathbf{P}_k^{x,u})^{-1} (\mathbf{I} - \mathbf{L}_k \mathbf{C}_k) \bar{\mathbf{A}}_{k-1} \bar{\mathbf{\Gamma}}_{k-1} > 0. \end{aligned} \quad (\text{A.5})$$

Since $\gamma_{k-1}^x \bar{\mathbf{B}}_{k-1}$ is a positive definite matrix, and $\|\boldsymbol{\alpha}_{k-1}\| \leq 1$, we have

$$\begin{aligned} \mathbf{I} - \gamma_{k-1}^x \bar{\mathbf{B}}_{k-1} &\leq \mathbf{\Gamma}_{k-1} \\ &= \mathbf{I} - \gamma_{k-1}^x \bar{\mathbf{B}}_{k-1} + \boldsymbol{\alpha}_{k-1} \gamma_{k-1}^x \bar{\mathbf{B}}_{k-1} \leq \mathbf{I}, \end{aligned}$$

which implies $\|\mathbf{\Gamma}_{k-1}\| \leq 1$. Since $\|\bar{\mathbf{\Gamma}}_{k-1}\| = 1$ and $\|\mathbf{\Gamma}_{k-1}\| \leq 1$, inequality (A.5) proves the claim. \square

Claim 11 *There exists a positive constant $c \triangleq \frac{\bar{p}(1 + \bar{l}\bar{c}_y)^2 (1 + \bar{g}\bar{m}\bar{c}_2)^2 \bar{q}}{\bar{p}(\bar{l}\bar{c}_y \bar{g}\bar{m} - \bar{l} - \bar{g}\bar{m})^2 \bar{r}_2} \text{rank}(\mathbf{Q}_{k-1}) + \bar{p}(\bar{l}\bar{c}_y \bar{g}\bar{m} - \bar{l} - \bar{g}\bar{m})^2 \bar{r}_2 \text{rank}(\mathbf{R}_k)$, such that*

$$\begin{aligned} \mathbb{E}[\|(\mathbf{I} - \mathbf{L}_k \mathbf{C}_k)^\top (\mathbf{P}_k^{x,u})^{-1} (\mathbf{I} - \mathbf{L}_k \mathbf{C}_k)\| \|\bar{\mathbf{w}}_{k-1}\|^2] \\ + \mathbb{E}[\|\bar{\mathbf{L}}_k (\mathbf{P}_k^{x,u})^{-1} \bar{\mathbf{L}}_k\| \|\mathbf{v}_k\|^2] \leq c. \end{aligned}$$

Proof: *The first term is bounded by*

$$\begin{aligned} \mathbb{E}[\|(\mathbf{I} - \mathbf{L}_k \mathbf{C}_k)^\top (\mathbf{P}_k^{x,u})^{-1} (\mathbf{I} - \mathbf{L}_k \mathbf{C}_k)\| \|\bar{\mathbf{w}}_{k-1}\|^2] \\ = \mathbb{E}[\|(\mathbf{I} - \mathbf{L}_k \mathbf{C}_k)^\top (\mathbf{P}_k^{x,u})^{-1} (\mathbf{I} - \mathbf{L}_k \mathbf{C}_k)\| \\ \|(\mathbf{I} - \mathbf{G}_{k-1} \mathbf{M}_k \mathbf{C}_k)\|^2 \|\mathbf{w}_{k-1}\|^2] \\ \leq \bar{p}(1 + \bar{l}\bar{c}_y)^2 (1 + \bar{g}\bar{m}\bar{c}_2)^2 \bar{q} \text{rank}(\mathbf{Q}_{k-1}), \end{aligned}$$

where we apply $\|\mathbf{w}_{k-1}\|^2 = \text{tr}(\mathbf{w}_{k-1} \mathbf{w}_{k-1}^\top) \leq \bar{q} \text{rank}(\mathbf{Q}_{k-1})$. Likewise, the second term is bounded by

$$\begin{aligned} \mathbb{E}[\|\bar{\mathbf{L}}_k (\mathbf{P}_k^{x,u})^{-1} \bar{\mathbf{L}}_k\| \|\mathbf{v}_k\|^2] \\ \leq \bar{p}(\bar{l}\bar{c}_y \bar{g}\bar{m} + \bar{l} + \bar{g}\bar{m})^2 \bar{r}_2 \text{rank}(\mathbf{R}_k). \end{aligned}$$

These complete the proof. \square

Through Claims 10 and 11, (A.2) becomes

$$\mathbb{E}[V_k] \leq \delta \mathbb{E}[V_{k-1}] + c.$$

By recursively applying the above relation, we have

$$\begin{aligned}\mathbb{E}[V_k] &\leq \delta^k \mathbb{E}[V_0] + \sum_{i=0}^{k-1} \delta^i c \leq \delta^k \mathbb{E}[V_0] + \sum_{i=0}^{\infty} \delta^i c \\ &= \delta^k \mathbb{E}[V_0] + \frac{c}{1-\delta},\end{aligned}$$

which implies practical exponential stability of the estimation error

$$\begin{aligned}\mathbb{E}[\|\tilde{\mathbf{x}}_k^u\|^2] &\leq \frac{\bar{p}}{p} \delta^k \mathbb{E}[\|\tilde{\mathbf{x}}_0^u\|^2] + \frac{c\bar{p}}{(1-\delta)} \\ &= a'_x e^{-b'_x k} \mathbb{E}[\|\tilde{\mathbf{x}}_0^u\|^2] + c'_x,\end{aligned}$$

where $(\tilde{\mathbf{x}}_k^u)^\top (\mathbf{P}_k^x)^{-1} (\tilde{\mathbf{x}}_k^u) \geq \lambda_{\min}((\mathbf{P}_k^x)^{-1}) \|\tilde{\mathbf{x}}_k^u\|^2 \geq \frac{1}{\bar{p}} \|\tilde{\mathbf{x}}_k^u\|^2$ and $(\tilde{\mathbf{x}}_0^u)^\top (\mathbf{P}_0^x)^{-1} \tilde{\mathbf{x}}_0^u \leq \lambda_{\max}((\mathbf{P}_0^x)^{-1}) \|\tilde{\mathbf{x}}_0^u\|^2 \leq \frac{1}{\underline{p}} \|\tilde{\mathbf{x}}_0^u\|^2$ have been applied. Constants are defined by

$$a'_x \triangleq \frac{\bar{p}}{\underline{p}}, \quad b'_x \triangleq \ln\left(1 + \frac{q'}{h^2 \bar{a}^2 \bar{p}}\right) \quad c'_x \triangleq \frac{c\bar{p}}{(1-\delta)}.$$

Since $\tilde{\mathbf{x}}_k$ is a linear transformation of $\tilde{\mathbf{x}}_k^u$, the same stability holds for $\tilde{\mathbf{x}}_k$. Likewise, the same stability holds for $\tilde{\mathbf{d}}_k$ in (15) because it is a linear transformation of $\tilde{\mathbf{x}}_k$. We omit its details. ■

References

- Anderson, B.D.O., Moore, J.B., 1981. Detectability and stabilizability of time-varying discrete-time linear-systems. *SIAM Journal on Control and Optimization* 19, 20–32.
- Barnard, G.A., 1959. Control charts and stochastic processes. *Journal of the Royal Statistical Society. Series B (Methodological)*, 239–271.
- Cárdenas, A.A., Amin, S., Sastry, S., 2008. Research challenges for the security of control systems. *HotSec* 5, 15.
- Cardenas, A.A., Amin, S., Sastry, S., 2008. Secure control: Towards survivable cyber-physical systems, in: 28th International Conference on Distributed Computing Systems Workshops, pp. 495–500.
- Checkoway, S., McCoy, D., Kantor, B., Anderson, D., Shacham, H., et al., 2011. Comprehensive experimental analyses of automotive attack surfaces, in: *USENIX Security Symposium*, pp. 447–462.
- Djouadi, S.M., Melin, A.M., Ferragut, E.M., Laska, J.A., Dong, J., Drira, A., 2015. Finite energy and bounded actuator attacks on cyber-physical systems, in: *IEEE European Control Conference (ECC)*, pp. 3659–3664.
- Fawzi, H., Tabuada, P., Diggavi, S., 2014. Secure estimation and control for cyber-physical systems under adversarial attacks. *IEEE Transactions on Automatic Control* 59, 1454–1467.
- Forti, N., Battistelli, G., Chisci, L., Sinopoli, B., 2016. A Bayesian approach to joint attack detection and resilient state estimation, in: *IEEE Conference on Decision and Control (CDC)*, pp. 1192–1198.
- Jafarnejadsani, H., Lee, H., Hovakimyan, N., Voulgaris, P., 2018. A multirate adaptive control for MIMO systems with application to cyber-physical security, in: *IEEE Conference on Decision and Control (CDC)*, pp. 6620–6625.
- Julier, S.J., LaViola, J.J., 2007. On Kalman filtering with nonlinear equality constraints. *IEEE Transactions on Signal Processing* 55, 2774–2784.
- Kafash, S.H., Giraldo, J., Murguia, C., Cardenas, A.A., Ruths, J., 2018. Constraining attacker capabilities through actuator saturation, in: *IEEE American Control Conference (ACC)*, pp. 986–991.
- Kim, H., Guo, P., Zhu, M., Liu, P., 2017. Attack-resilient estimation of switched nonlinear cyber-physical systems, in: *IEEE American Control Conference (ACC)*, pp. 4328–4333.
- Kim, H., Guo, P., Zhu, M., Liu, P., 2020. Simultaneous input and state estimation for stochastic nonlinear systems with additive unknown inputs. *Automatica* 111, 108588.
- Kluge, S., Reif, K., Brokate, M., 2010. Stochastic stability of the extended Kalman filter with intermittent observations. *IEEE Transactions on Automatic Control* 55, 514–518.
- Ko, S., Bitmead, R.R., 2007. State estimation for linear systems with state equality constraints. *Automatica* 43, 1363–1368.
- Kong, J., Pfeiffer, M., Schildbach, G., Borrelli, F., 2015. Kinematic and dynamic vehicle models for autonomous driving control design, in: *IEEE Intelligent Vehicles Symposium (IV)*, pp. 1094–1099.
- Koscher, K., Czeskis, A., Roesner, F., Patel, S., Kohno, T., Checkoway, S., McCoy, D., Kantor, B., Anderson, D., Shacham, H., et al., 2010. Experimental security analysis of a modern automobile, in: *IEEE Symposium on Security and Privacy*, pp. 447–462.
- Lai, T.L., 1995. Sequential changepoint detection in quality control and dynamical systems. *Journal of the Royal Statistical Society. Series B (Methodological)*, 613–658.
- Langner, R., 2011. Stuxnet: Dissecting a cyber warfare weapon. *IEEE Security & Privacy* 9, 49–51.
- Law, C.K., Dalal, D., Shearow, S., 2018. Robust model predictive control for autonomous vehicles/self driving cars. *arXiv preprint arXiv:1805.08551*.
- Lee, R.M., Assante, M.J., Conway, T., 2014. German steel mill cyber attack. *Industrial Control Systems* 30, 22.
- Liu, Y., Ning, P., Reiter, M.K., 2011. False data injection attacks against state estimation in electric power grids. *ACM Transactions on Information and System Security* 14, 21–32.
- Mo, Y., Chabukswar, R., Sinopoli, B., 2014. Detecting integrity attacks on SCADA systems. *IEEE Transactions on Control Systems Technology* 22, 1396–1407.

- Mo, Y., Sinopoli, B., 2009. Secure control against replay attacks, in: 47th Annual Allerton Conference on Communication, Control, and Computing, pp. 911–918.
- Mourikis, A.I., Roumeliotis, S.I., 2007. A multi-state constraint Kalman filter for vision-aided inertial navigation, in: IEEE International Conference on Robotics and Automation (ICRA), pp. 3565–3572.
- Page, E.S., 1954. Continuous inspection schemes. *Biometrika* 41, 100–115.
- Pajic, M., Lee, I., Pappas, G.J., 2017. Attack-resilient state estimation for noisy dynamical systems. *IEEE Transactions on Control of Network Systems* 4, 82–92.
- Pajic, M., Weimer, J., Bezzo, N., Tabuada, P., Sokol-sky, O., Lee, I., Pappas, G.J., 2014. Robustness of attack-resilient state estimators, in: ACM/IEEE International Conference on Cyber-Physical Systems, pp. 163–174.
- Papoulis, A., Pillai, S.U., 2002. Probability, random variables, and stochastic processes. Tata McGraw-Hill Education.
- Pasqualetti, F., Dörfler, F., Bullo, F., 2013. Attack detection and identification in cyber-physical systems. *IEEE Transactions on Automatic Control* 58, 2715–2729.
- Peterson, S., Faramarzi, P., 2011. Iran hijacked us drone, says iranian engineer. *Christian Science Monitor* 15.
- Raiyn, J., 2014. A survey of cyber attack detection strategies. *International Journal of Security and Its Applications* 8, 247–256.
- Rajamani, R., 2011. Vehicle dynamics and control. Springer Science & Business Media.
- Rajkumar, R., Lee, I., Sha, L., Stankovic, J., 2010. Cyber-physical systems: the next computing revolution, in: IEEE Design Automation Conference, pp. 731–736.
- Sayed, A.H., 2003. Fundamentals of adaptive filtering. John Wiley & Sons.
- Simon, D., 2010. Kalman filtering with state constraints: A survey of linear and nonlinear algorithms. *IET Control Theory & Applications* 4, 1303–1318.
- Simon, D., Chia, T.L., 2002. Kalman filtering with state equality constraints. *IEEE Transactions on Aerospace and Electronic Systems* 38, 128–136.
- Slay, J., Miller, M., 2007. Lessons learned from the Maroochy water breach, in: Springer International Conference on Critical Infrastructure Protection, pp. 73–82.
- Teixeira, A., Amin, S., Sandberg, H., Johansson, K.H., Sastry, S.S., 2010. Cyber security analysis of state estimators in electric power systems, in: IEEE Conference on Decision and Control (CDC), pp. 5991–5998.
- Teixeira, A., Pérez, D., Sandberg, H., Johansson, K.H., 2012. Attack models and scenarios for networked control systems, in: Proceedings of the 1st international conference on High Confidence Networked Systems, pp. 55–64.
- Teixeira, A., Shames, I., Sandberg, H., Johansson, K.H., 2015. A secure control framework for resource-limited adversaries. *Automatica* 51, 135–148.
- Tylavsky, D.J., Sohie, G.R., 1986. Generalization of the matrix inversion lemma. *Proceedings of the IEEE* 74, 1050–1052.
- Wan, W., Kim, H., Hovakimyan, N., Voulgaris, P.G., 2019. Attack-resilient estimation for linear discrete-time stochastic systems with input and state constraints, in: IEEE Conference on Decision and Control (CDC), pp. 5107–5112.
- Wang, L., Chiang, Y., Chang, F., 2002. Filtering method for nonlinear systems with constraints. *IEEE Proceedings-Control Theory and Applications* 149, 525–531.
- Wood, A.J., Wollenberg, B.F., Sheblé, G.B., 2013. Power generation, operation, and control. John Wiley & Sons.
- Yong, S.Z., Zhu, M., Frazzoli, E., 2015a. Resilient state estimation against switching attacks on stochastic cyber-physical systems, in: IEEE Conference on Decision and Control (CDC), pp. 5162–5169.
- Yong, S.Z., Zhu, M., Frazzoli, E., 2015b. Simultaneous input and state estimation of linear discrete-time stochastic systems with input aggregate information, in: IEEE Conference on Decision and Control (CDC), pp. 461–467.
- Yong, S.Z., Zhu, M., Frazzoli, E., 2016. A unified filter for simultaneous input and state estimation of linear discrete-time stochastic systems. *Automatica* 63, 321–329.